Dynamic Hardness Testing Challenges Conventional Tests

by

54

Walter Kohlhöfer

B.Sc. (Eng)(Mech) UCT

A thesis submitted in fulfillment of the requirements for the degree of Master of Science in Engineering

Department of Mechanical Engineering
University of Cape Town

June 1993

Declaration

This is to certify that the results, calculations and any other work presented in this thesis are essentially my own work, and that no part of it has been submitted for a degree at any other university.

Signed by candidate

Walter Kohlhöfer
June 1993

Acknowledgements

I acknowledge, and sincerely appreciate, the help and support of the following people:

Professor R. K. Penny for his supervision, guidance and support.

Professor G Gryzagoridis for his encouragement when problems arose.

Professor Bell of Electrical Engineering for his help in determining the Young's moduli of the specimens.

Martin Batho, Arnold Warburton and Horst Emrich for their help in manufacturing specimens and hardware.

Julian Meyer for his help with the electronics.

The staff of the workshop for their help in manufacturing specimens and also for their moral support.

Fellow students for their support and company.

Family and friends for their financial and moral support.

ABSTRACT

The design and use of a portable dynamic hardness tester is described. The thesis begins with a description of the more common static hardness tests and the usefulness of such tests in industry. It shows a correlation between the different types of hardness and also between hardness and other material parameters such as tensile strength. A thorough investigation of the principles involved in the indentation processes using conical and spherical indenters under static and dynamic loading is given so that the reasons for the correlations may be more clearly understood. A series of test specimens tested by conventional static hardness tests (Brinell, Vickers and Rockwell) are used as calibration specimens for the dynamic tester. Both a spherical and conical tip are used. The results of these tests are compared and analyzed. The dynamic tester may then be programmed so that it correlates with the results of the static tests. A set of guidelines for the use of such a portable tester is then given.

TABLE OF CONTENTS

1. INTRODUCTION

Practically all branches of engineering, especially those dealing with structures and machines are closely concerned with materials, the properties of which must be determined by tests. Successful mass production depends upon inspection and quality control of manufactured products. The preparation of adequate specifications and the acceptance of materials purchased under specifications involve the understanding of test methods and of inspection. Engineering research and development function, in large measure, on an experimental basis and call for carefully planned, well devised tests. The hardness test is one which may be applied to the above situations. Due to its inherent simplicity, it should be further researched to ascertain its possible usefulness to determine other properties such as fatigue life and wear for example.

The hardness test which measures the mean contact pressure when a spherical, conical or pyramidal indenter is pressed into the surface of a flat specimen, provides a very simple and non destructive means for assessing the resistance of a material to plastic deformation.

Although hardness tests may appear different in procedure, eg. static or dynamic, conical or spherical indenter, the equivalent plastic flow stress Y of the material is a common factor. Most existing hardness tests have inherent disadvantages; the greatest of these is that one test cannot cover the entire range of hardness values without either changing the indenter or, the applied load.

Much of the discussion to follow is concerned with relating the hardness values obtained from different testing machines to the flow stress of the material as measured in the tension or compression test. This not only gives insight into the hardness testing procedures, but makes it possible to derive conversion equations which relate one hardness test to another.

With respect to the usability of a part after a test, the tests may be classified as *destructive* or *nondestructive*. Tests to determine ultimate strength mean destruction of a sample. Since an entire lot cannot be sampled, there enter problems obtaining a reliable indication of strength of the lot by using a sufficient number of samples. For finished products it is desirable to use nondestructive tests if possible. Some

hardness tests, eg. the dynamic test, may be classified into this category. If the hardness test may thus be applied to determine the ultimate strength for example, such samples may be tested without destruction.

2. STATEMENT OF OBJECTIVES

The aims and objectives of this dissertation are briefly stated below:

- To discover any common features between well - known hardness measures (principally those of Brinell, Vickers and Rockwell) and give their advantages and limitations.

- To correlate the hardness tests and show their suitability for different applications.

- To relate through mechanics, the measures obtained from static tests to those obtained from dynamic tests.

- To combine relevant results obtained into the design of a portable, dynamic hardness tester and to show how the results correlate with static tests.

3. LITERATURE SURVEY

3.1. Stress and Strain - A General Overview

When designing for operating loads, component dimensions and stresses need to be related in order to decide on suitable working stress values. In this chapter, the basic forms of stress are discussed in relation to external factors (forces) and internal stresses and strains. These relationships are vital for an insight into component behaviour.

It is interesting to note that stress is not a physical, measurable parameter, but only a mathematical tool relating loading to geometry. Strain, on the other hand, is a physical measure. When a bar is subjected to tension, it is elongated. The amount of elongation is related to the original dimensions of the bar by a measure called strain.

3.1.1. Ideal Plastic Materials

In the formation of an indentation made by any hardness tester, one is concerned mainly with the plastic flow of metal around the indenter. For this reason it is necessary to discuss the nature of plastic deformation.

Suppose one takes a uniform cylinder and subjects it to a tensile or compressive force along its axis. One then measures its deformation. In other words, the strain is a function of the deforming stress. The stress may be defined in two ways. The nominal stress is the tensile or compressive force divided by the original cross-sectional area of the specimen. On the other hand, the true stress is the tensional or compressive force divided by the area of the specimen at that stage of deformation, i.e.

True Stress = load / current cross-sectional area (3.1)

Nominal Stress = load / original cross-sectional area (3.2)

Strain may also be defined in various ways. For small deformations the linear strain is the fractional increase in length of a specimen, so that if l_0 is the original length and l the length at any later stage, then,

$$\epsilon = (l - l_0)/l_0 \qquad (3.3)$$

For a tensile force, ϵ is positive, for a compressive force, it is negative. One may also use the cross-sectional areas A_0 and A instead of the lengths to calculate the strain. Since there is a negligible amount of volume change in plastic deformation, $l_0 A_0 = l A$ = constant, so that for plastic deformation,

$$\epsilon = (l - l_0)/l_0 = \frac{A_0 l - A l}{A l} = \frac{A_0 - A}{A} \qquad (3.4)$$

For most purposes, it is sufficient to use linear strain and this will be used in the following discussion of stress-strain curves under tension and compression.

The term true stress is used to indicate the result obtained when any load used in the tensile test is divided by the true or actual cross sectional area of the specimen. This means that both the load and cross sectional area must be measured simultaneously during the test. In plotting the true stress strain diagram, it is customary to use a term called true strain, sometimes called logarithmic strain. True strain is the sum of each incremental elongation divided by the current length of the filament, or

$$\xi = \ln(l / l_0) \qquad (3.5)$$

The relationship between linear and logarithmic strain may be obtained by rearranging equation 3.4 to:

$$\epsilon = (l - l_0)/l_0 = (l / l_0) - 1 \qquad (3.6)$$

and hence:

$$\epsilon + 1 = (l / l_0) \qquad (3.6a)$$

and so, from equation 3.5:

$$\xi = \ln(\epsilon + 1) \tag{3.7}$$

3.1.2. True Stress - Strain Curves under Tension

Firstly, one must consider the behaviour of an elastic, perfectly plastic material under tension and plot the linear strain ϵ as a function of the true stress σ.

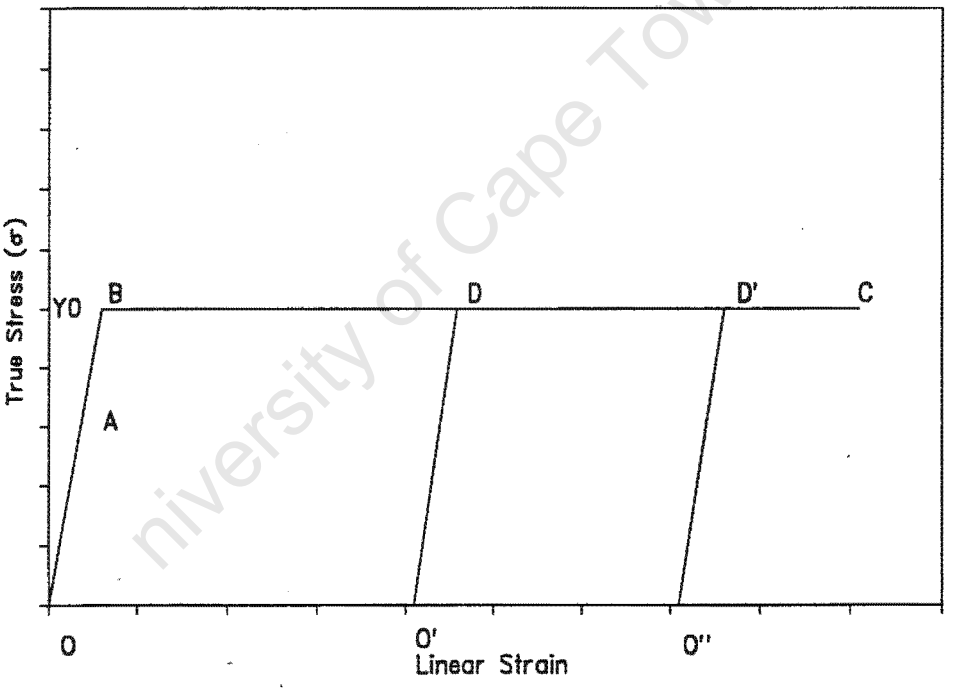

Figure 3.1 True Stress-Strain Curve

At first, there will be a slight increase in the length, which is proportional to the load applied. Over this range, Hooke's law is obeyed and the deformation is purely elastic and upon releasing the load, the cylinder will return to its original length ($O\,A$). The slope of the line $O\,A$ is the ratio of stress to strain and is termed the Young's modulus of the metal. When the load reaches a certain level, the cylinder will increase in length and this increase will be non - reversible. The stress at which this occurs is called

yield stress Y_0. If the material does not work - harden, that is, if the stress remains constant during the extension, the stress strain curve is a straight line *B C* and is parallel to the strain axis. If at any point D, the load is reduced, the cylinder contracts elastically along the line *D O'*, where this is approximately parallel to *A O*. If the load is completely removed, the cylinder will have undergone permanent deformation *O O'*. On increasing the load again, the deformation will proceed elastically along *O' D* and then deform plastically further along *D C*. Metals which have a constant *Y* and have a similar stress - strain curve as shown in figure 3.1 are called ideal plastic materials (perfectly elastic - plastic). No real metals have these properties, but it is possible to obtain a close approximation to them, eg. structural steel. In practice all metals work - harden at some stage as a result of the deformation, and the stress - strain curve is of the type shown in figure 3.2.

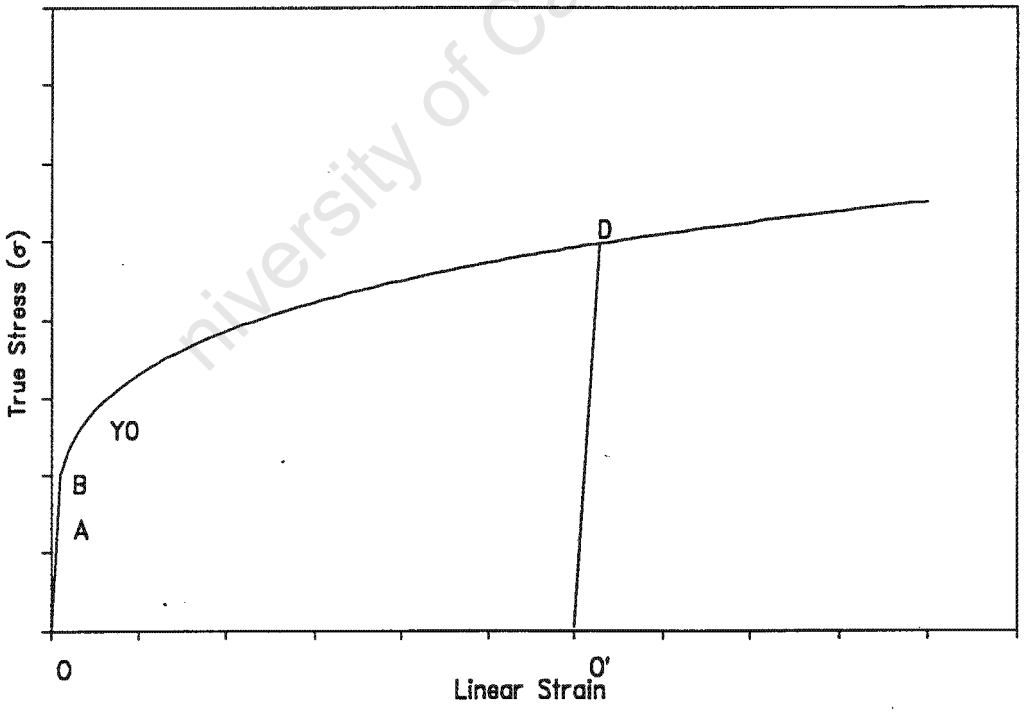

Figure 3.2 True stress - strain curve of a metal which work - hardens

Once plastic yielding has occurred, the stress required to produce further yielding increases rapidly at first and then gradually. Thus at any point *D* the stress required to produce further plastic flow is no longer the initial

yield stress Y_0 but a larger stress, so that the yield stress varies with the amount of deformation. With many metals, the dependence of yield stress Y on the deformation ϵ may be approximated by the equation $Y = b\,\epsilon^{x}$ [Nadai, 1931]. If at point D the stress is removed, the specimen contracts elastically along $D\,O'$.

3.2. Applications of Hardness

Hardness tests have a wide field of use, although as commercial tests they are perhaps more commonly used on metals than any other class of materials. The results of hardness tests may be used as follows:

- Similar materials may be graded according to hardness, and a particular grade may be specified for some one type of service. The degree of hardness chosen depends, however, on previous experience with materials under the given service, and not upon any intrinsic significance of the hardness numbers. It should be noted that the observed hardness number cannot be utilized directly in design or analysis as can tensile strength, for example.

- The quality level of materials or products may be checked or controlled by hardness tests. They may be applied to determine the uniformity of samples of a metal or the uniformity of results of some treatment such as forming, heat treating or alloying.

- By establishing a correlation between hardness and some other desired property, e.g., tensile strength, simple hardness tests may serve to control the uniformity of the of the tensile strength and to indicate rapidly whether more complete tests are warranted. It should be noted, however, that correlation apply only over a range of materials on which tests have previously been made; extrapolations from empirical relations should only be made with extreme caution.

Since Brinell [Brinell, 1900] established his empirical relationship between hardness and tensile strength, the idea of obtaining mechanical properties,

for example, tensile strength, yield stress, percentage elongation [Böklen, 1971] and the fatigue life [O'Niell, 1967] by a simple indentation will remain the aim of technological investigations concerned with hardness in a general sense. Recently, the hardness test has become a popular tool for use in Non Destructive Evaluation Procedures [Au et al., 1980]. These can be invaluable in the early stages of materials characterisation, particularly for materials required to operate at high temperatures, or during creep. With improved measuring techniques and better understanding of the mechanics of the hardness test, the range of usefulness of these tests has increased.

3.2.1 Relating Hardness to Tensile Strength

In the solid state the cohesive and adhesive forces are so strong that the atoms retain fixed positions relative to each other. This produces an aggregate that has and retains definite form. Resistance to change in form, ie., to change of relative positions of the atoms composing a body, may be defined as the rigidity of that material. The stress necessary to produce permanent deformation of the structure of the solid is most intimately allied to the property of hardness, for, in the measurement of hardness by a penetration method, it will be necessary to vary permanently these fixed positions that the atoms bear with respect to each other [Williams, 1942].

Due to the similarity in the inelastic strain involved in the test for ultimate tensile strength and indentation hardness, empirical relations have been developed between the two properties for certain steels.

When a plastic indentation is produced in a material, some permanent strain is suffered as a consequence of the deformation. The plastic strain field around any indentation will in general be complicated and vary from point to point, but one can talk in terms of a *representative strain*, characteristic of the indenter and loading conditions [Atkins & Tabor, 1965]. Where geometric similarity holds, this representative strain will be independent of the size of the indentation; this is true for a wedge, cone and pyramidal indentations.

It is known that for fully work hardened materials the indentation hardness is a certain multiple of the yield stress of that material. One may write $P_m = c\ Y$, where P_m is the hardness, Y the yield stress, and c the constant of proportionality, which depends on the geometry of the indenter [Tabor, 1951].

3.2.2 Determining Stress Strain from Hardness

Although the Meyer hardness number is discussed fully, later in this chapter, it is used here to show the relation between hardness and the stress - strain characteristic.

If a ball indenter of diameter D is pressed into a specimen by a load W, it will give rise to an interfacial pressure P_m which is given by:

$$P_m = \frac{4\ W}{\pi\ d^2} \tag{3.8}$$

where d is the chordal diameter of the indentation. For light loads, this in turn develops a purely elastic stress field in both the specimen and indenter [Hertz, 1881]. Upon load removal, the elastic stress field recovers and no permanent indentation remains. If the load is increased, a point will be reached at which material in the specimen will begin to flow plastically in a small zone, the plastic zone, below the surface of the indenter [Hertz, 1881]. At the point at which the plastic zone initiates it has been shown that [Tabor, 1951]:

$$P_m = 1.07\ \sigma_t \tag{3.9}$$

where σ_t is the true uniaxial flow stress of the specimen below the indenter.

If the load applied is increased further, the plastic zone will grow and it will ultimately intersect the surface of the specimen. once it has been fully developed, it has been shown that [Shaw & De Salvo, 1970]:

$$P_m \approx 2.8\ \sigma_t \tag{3.10}$$

That is, the ratio of P_m / σ_t remains constant with increasing loads.

As mentioned previously, in the event that plastic deformation occurs during penetration a permanent indentation is left after load removal. A small shoulder develops around the edge of the indentation, and that as a result of the elastic stress recovery, the permanent indentation has a larger radius of curvature than the indenter.

Several investigations have correlated geometric features of the indentations with effective true plastic strains ϵ_p [Tabor, 1951, Francis, 1976]. The values of ϵ_p referred to here are those which would correspond to a value of σ_t in a uniaxial tensile stress - strain relationship. In particular, Tabor demonstrated empirically that such a value of ϵ_p is given by [Tabor, 1951]:

$$\epsilon_p = 0.2 \ d/D \tag{3.11}$$

Recently, Cahoon [Cahoon, 1972] presented an improved equation relating hardness to ultimate tensile strength of metals and alloys. The equation is given as:

$$\sigma_u = \frac{H}{2.9}\left[\frac{n}{0.217}\right] \tag{3.12}$$

Where σ_u is the ultimate nominal stress, H is the Vickers hardness and n the strain hardening coefficient as related by the familiar equation,

$$\sigma = k \epsilon^n \tag{3.13}$$

with σ and ϵ being the true stress and true strain in the plastic region. The constant k generally is called the strength coefficient. The improved equation is derived in a manner similar to earlier work [Tabor, 1951]. Work carried out by Moteff et al. [Moteff, 1984] showed that this correlation is also true for experiments where the hardness and tensile tests are carried out at elevated temperatures.

3.2.3 Relating Hardness to Creep

An investigation on CrMoV rotors [Kimura et al, 1990] revealed that typical material degradation was softening and excellent correlations between hardness and creep properties were observed and general equations which correlate hardness and creep properties were proposed.

Creep rupture life as represented by the Larson - Miller parameter P is shortened when the hardness is lowered or the stress is increased. Kimura et al carried out creep rupture tests after they had performed Vickers tests on the specimens. They found that the relationship between creep rupture life (P) and Vickers hardness (Hv) could be fitted by a straight line and if the stress is fixed, P becomes smaller as hardness decreases.

$$P = \{A\,\sigma\}\,Hv + \{B\,\sigma\} \qquad (3.14)$$

Where A σ and B σ are functions of stress only.

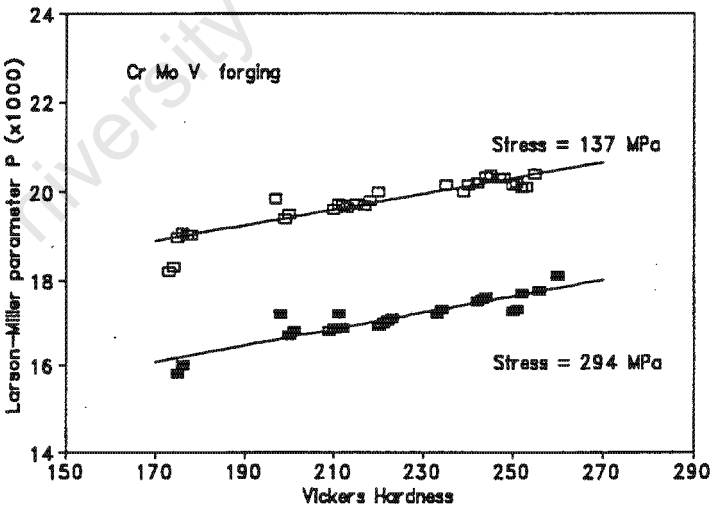

Fig 3.3 Hardness dependence of creep rupture life

Remnant creep life assessment of pressure vessels, based on hardness measurements has also been suggested [Cane et al., 1985]. It is known that structural coarsening fo the low alloy ferritic steels is the cause of the continuous reduction in the creep strength during service exposure.

Although the model suggested by Cane et al. quantifies the structural coarsening, it is often difficult to measure the interparticle spacing. In order for the measurements to be objective, it is necessary to sample large populations, coupled with careful replication procedures. They therefore suggest an alternative approach where the microstructural degradation is quantified by hardness measurements. Figure 3.4 shows an example of the correlation between hardness and interparticle spacing.

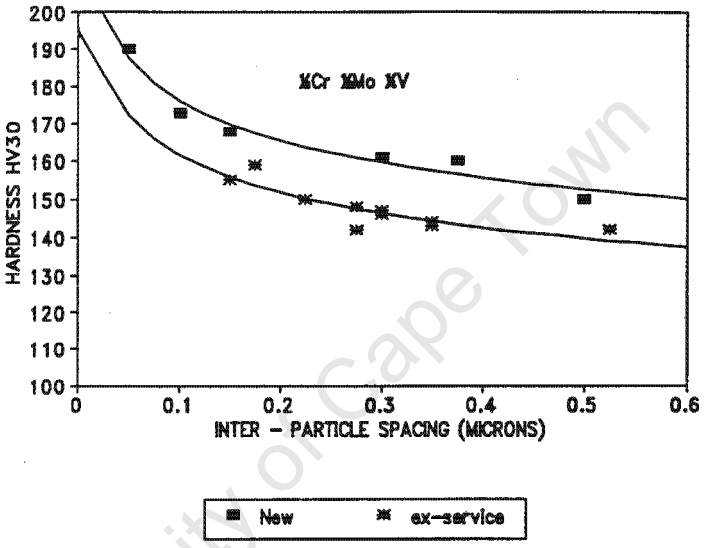

Fig 3.4 Relationship between hardness and interparticle spacing

3.2.4 Relating Hardness to Fatigue Life

Because fatigue is associated with plastic deformation, one would first of all expect that the resistance to fatigue would be related to resistance to plastic deformation. However, the fatigue strength seems to be more closely correlated to tensile strength than any other single physical property since it is a progressive fracture [Davis, Troxel & Wiskocil, 1964]. The Brinell hardness test seems to furnish a fair index of the endurance limit for most steels. The endurance limit is about 250 times the Brinell hardness number. This is to be expected since it was shown above that tensile strength may be related to hardness and hence it follows that fatigue strength must also be related.

3.3. Hardness - A Definition

Hardness is a term which has different meanings in different situations. It may mean a resistance to penetration [Davis et al, 1964], resistance to wear [Lipson, 1967], or a measure of flow stress [O'Neill, 1967]. Although these actions appear different in character, they are all related to the plastic flow of the material. The two hardness tests investigated by the author are:

1. Indentation hardness - Resistance to permanent deformation due to static or dynamic loads.

2. Rebound hardness - Energy absorption under impact loads.

The hardness of a material may be expressed in terms of the elastic and plastic properties of that material. This indicates that there is a relation between the hardness and other material properties: eg. yield strength. The different hardness tests use indenters of differing shapes and thus do not cause the same flow of material around the indenter. Thus no one hardness test uniquely indicates any other material property.

3.4. Introduction to Hardness Tests

The resistance to indentation is used as the basis for a variety of hardness tests. The indenter, (a ball, a plain or truncated cone, a pyramid) is usually made of hard steel or diamond and used under a static or dynamic load. The depth of indentation for a given load or the load required to give a set indentation could be measured. The measured variable is then a function of the hardness.

In the case of dynamic rebound hardness tests, the height of rebound of the indenter is a measure of hardness. The rebound is due to the release of elastic energy of the bulk material and thus does not depend on the plastic flow of the material to the same extent as the static tests. One would thus expect the relation between hardness and other material properties to be more accurate. The following section of the thesis briefly describes the common types of hardness tests and the differences between them.

3.5. Static Indentation Hardness Tests

The static indentation hardness of materials may be expressed in terms of the plastic and to a lesser degree, in terms of elastic properties of the material. Almost all indentation hardness testing is done with Brinell, Rockwell or Vickers indenters. These techniques are discussed further in this chapter.

Although the indentation tests are done using the testers mentioned above, additional equipment may be required. Composition, size and hardness of the test piece are important factors which govern the selection of the test equipment. Often the test piece may be brought to the tester, however, this is not always practical and so this thesis also deals with a portable dynamic hardness tester for such cases.

Indentation testing produces a depression on the surface. Although this does not usually impair serviceability, it may be a stress raiser in the part. Also, if surface finish is important, hardness testing may indeed be considered destructive testing. Static indentation tests also produce a zone of work hardening below the impression. This may adversely affect the fatigue strength of the part.

3.5.1. Brinell Hardness

In the Brinell Hardness Test [Brinell, 1900] (see also BS 240), a hard spherical indenter (of tungsten carbide) is pressed into the smooth surface of the test material. This occurs under a fixed normal load. The diameter of the remaining impression is then measured.

The Brinell Hardness is not a constant for a given metal, but depends on the load and the size of the indenter. However, if the indentations are geometrically similar (the ratio of the diameter of the indentation to the indenter diameter is constant), the hardness is constant. The hardness test uses the ratio of applied load to the curved surface area of the indentation. This is done to compensate for the work-hardening which might occur during the test. This concept gives rise to the misleading characteristic that

the Brinell Hardness Number (HB) is lower at higher loads than at smaller loads.

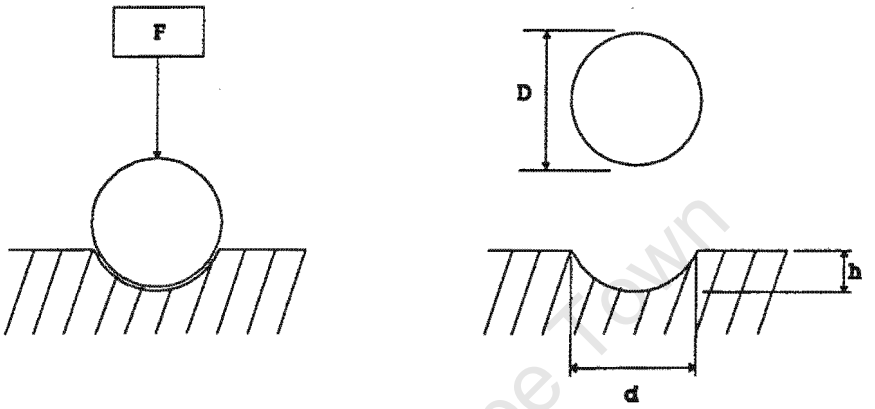

Figure 3.5 The Brinell Principle

$$HB = \frac{2 * LOAD}{\pi D^2\{1-\sqrt{[1-(d/D)^2]}\}} \qquad (3.15)$$

The Brinell hardness test has three principal limitations:

- The size and shape of the workpiece must be able to accommodate relatively large indentations.
- Due to the relatively large indentations, the workpiece may not be usable after testing, or may require corrective machining.
- The general hardness range of about 16 HB (500 kg load) to 630 HB (3000 kg load).

3.5.2. Meyer Hardness

This hardness test is based on the same principles as the Brinell Hardness Test. It differs in the fact that the projected surface area and not the curved surface area is used in the calculation of hardness. Thus this test makes use of the mean pressure over the surface area and this eliminates the problem of decreasing hardness with increasing load.

$$\text{Meyer Hardness} = \frac{4 * \text{LOAD}}{\pi d^2} \tag{3.16}$$

The relationship between load and size of indentation for spherical indenters may be expressed by an empirical relation. This is known as Meyer's law [Meyer 1908]. If the load applied is W and the chordal diameter of the remaining indentation is d then:

$$W = k\, d^{n} \tag{3.17}$$

where k and n are constants for the given material. The value of n usually lies between 2 and 2.5.

3.5.3. Vickers Hardness Test

In this test, a diamond indenter in the form of a right pyramid is forced under load into the test material. The geometry of the indenter is such that the base of the pyramid has an area equal to 0.927 times the surface area of the faces. Since the Vickers hardness number is defined as load divided by surface area, the yield pressure P is related to the Vickers hardness number by the relation:

$$H_V = 0.927\, P \tag{3.18}$$

The figure below shows the dimensions of the indentation. The mean of the two diagonals, d_1 and d_2 is calculated. This mean diameter d is used to calculate the surface area. If the indentation is square, the projected area of indentation is $d^2/2$ so that the yield pressure is (2 * Load) / d^2 and hence:

$$H_V = 0.927\ (2 * \text{LOAD} / d^2) \qquad (3.19)$$

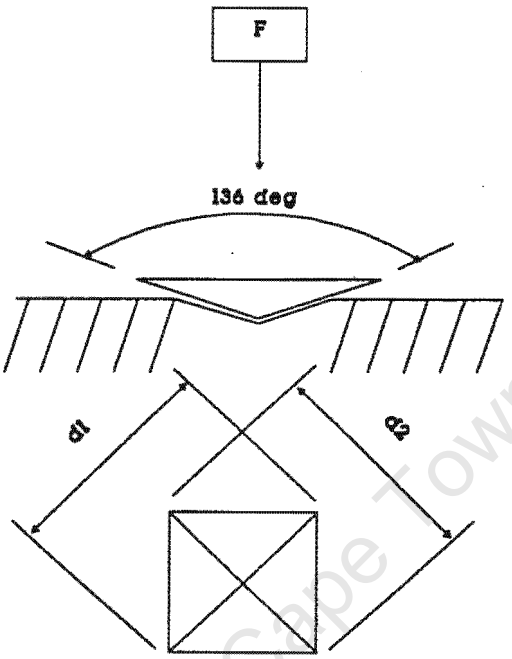

Figure 3.6 The Vickers Principle

Experiments have shown that the Vickers hardness number is independent of the size of indentation and therefore of the load. In this it differs from the Brinell test, but for a given load, the Brinell and Vickers numbers are in good correlation.

3.5.4. The Rockwell Test

In the Rockwell test [BS 891, 1962], the depth of the penetration is measured. In this way it differs from the previous tests mentioned. It is, however, similar to the Brinell and Vickers tests in that the hardness number is a function of the degree of indentation caused by the applied static load. For a softer metal, a spherical indenter is used (Rockwell B) and for harder metals, a conical indenter with a spherical tip (Rockwell C).

A feature of the Rockwell test is that a small load is first applied to cause an indentation This is used as the zero of further measurement when the larger

load is applied. The advantage of this is that the application and retention of the minor load prepares the surface upon which the increment in penetration due to the major load is based.

There is however a disadvantage to this test. The depth of the indentation is measured with the load applied. Due to elastic recovery of the metal, the depth of the recovered indentation after the load has been removed may be considerably less. This may introduce a considerable error and a correction of this is difficult as different materials have differing recovery rates.

The Monotron test [O'Neill, 1934] attempts to overcome this shortfall. Here the load to produce a certain set depth is measured.

Another source of error in the depth measuring technique is that of piling-up or sinking-in. This occurs when the material around the test area moves up the surface of the indenter, or the surrounding material sinks. However, as these effects are negligible, they do not constitute a serious error.

3.5.5. Comparison of Static Hardness Tests

Indentation tests not only differ with regard to the shape of the indenter, but in addition may also differ as follows:

- By use of a fixed load P, and measurement of the resulting diameter d, or width of impression at the surface (Brinell, Vickers).

- By using the contact area A_c in computing the mean unit load on the indenter, P / A_c, or by using the projected area of the impression, A.

- By use of a fixed load P, and measurement of the resulting depth of the impression t (Rockwell).

To eliminate the time required for microscopic observation of the indentation, the Rockwell test [Rockwell, 1922] was introduced. However, the Rockwell tests do not have the dimensions of force per unit area. In fact, the Rockwell number cannot be assigned any dimensions, since it is

defined in terms of an arbitrary equation. In order to use Rockwell numbers in engineering computations, they must first be converted to Brinell or Vickers hardness numbers which do have dimensions and physical significance.

Rockwell did an analysis to suggest such a conversion and then a more precise determination of the constants in this equation by the use of empirical data. His analysis yielded the following equation:

$$R_b = 130 - \frac{9000}{B} \tag{3.20}$$

He did however make several approximations in determining the relationship, and using data [de la Macorra, 1923], the more accurate coefficients are:

$$R_b = 134 - \frac{6700}{B} \pm 7 \tag{3.20a}$$

For conical indenters, an even cruder approximation shows that the relationship between Rockwell hardness and Brinell hardness may be given as:

$$R_c = 115 - \frac{1500}{\sqrt{B}} \tag{3.21}$$

Tabor [Tabor, 1951] suggested the coefficients to be 124 and 1510 respectively. The present author also performed the various types of hardness tests on the calibration specimens and determined the coefficients to be 120 and 1510. More accurate empirical conversion tables may be found in the SABS 055 - 1977.

Figure 3.7 shows a comparison between the various hardness values.

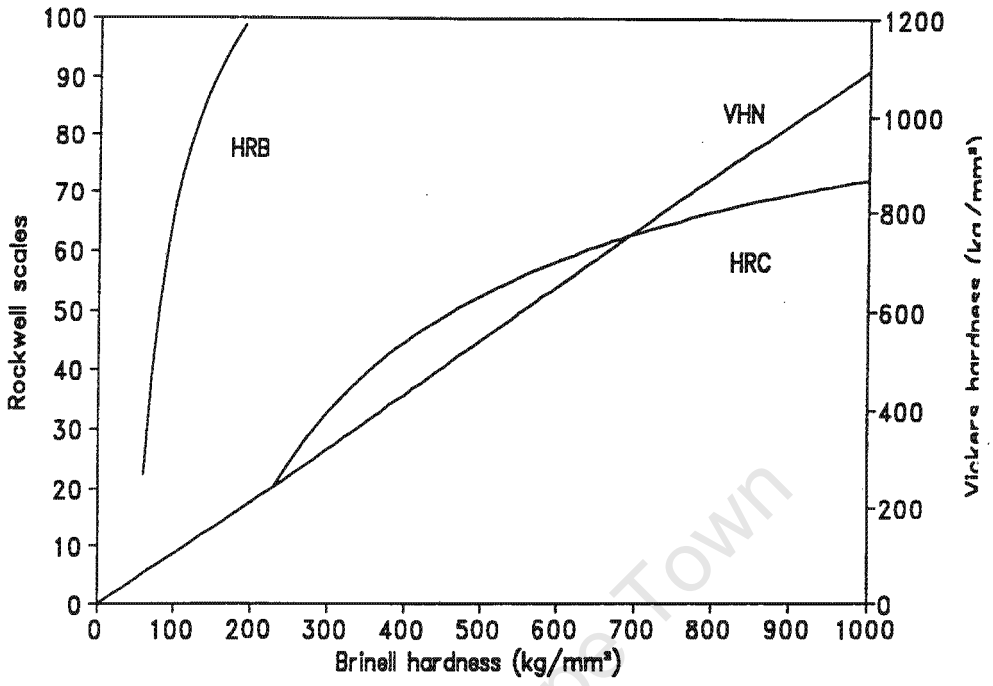

Fig 3.7 Hardness numbers as a function of Brinell hardness. Tungsten carbide ball used above 500 kg/mm² [McClintok & Argon 1966]

Conical or pyramidal indenters (Vickers and Rockwell) produce plastic flow at the tip of the indenter at very light loads. This is due to the fact that the tip is infinitely small. Thus the hardness number obtained from these tests has a single value over a wide range of loads. This fact makes them very convenient to use as careful load constraints are not critical.

For spherical indenters (Brinell) this is not the case. The yield pressure increases with the size of the indentation. This is due to the fact that the indentation changes shape as it varies in size. Thus, the yield pressure increases with the load. The load and indenter diameter must now be specified. This fact provides useful information about the elastic limit of the material.

Although these tests are more difficult to perform, they provide more information and thus the Brinell test, using the analysis of Meyer, may be used to examine the stress-strain characteristics of the material.

3.5.6. Selecting the Hardness Test

When selecting an appropriate hardness test, several factors should be taken into consideration [Jankowski, 1988]:

- Size and shape of the component. Small, complex parts require a tester with a small indenter to allow access.

- Material composition and microstructure. The hardness test method must be able to sample a representative area of the material. Coarse grained materials require either a hardness tester which measures a large indentation area, or multiple tests whose results may be averaged.

- Size of the tolerable indentation. Hardness testing for fine finished surfaces requires a test that is virtually nondestructive, i.e., does not leave an indentation which requires corrective machining.

In general, the large sampling area of the Brinell test limits its use to components with fairly simple geometries and large flat surfaces. Its main advantage is the ability to test components with rough surface finishes and coarse microstructures, such as steel forgings. The versatile Rockwell hardness test can be used to measure the hardness of a large number of different materials with varying compositions and microstructures. The small tip of the Rockwell indenter allows pin-point positioning to the desired test area. The Vickers test also shares these advantages with the Rockwell test.

3.6. Dynamic or Rebound Hardness Tests

The dynamic hardness may be defined as the resistance of a material to local deformation due to an impact load. If a spherical or conical indenter is used, and there is a constant dynamic pressure P resisting the indentation, the following equation holds

$$P = \text{energy of impact} / V \qquad (3.22)$$

where V is the volume of indentation. This pressure is sometimes called the dynamic hardness number.

3.6.1. Four Stages of Impact

Take the example where a spherical indenter is dropped onto the test specimen. The indenter strikes the surface and rebounds. The following four stages occur on impact. Firstly, the region of contact will deform elastically. Secondly, if the mean pressure of impact exceeds about $1.1Y$, where Y is the yield stress of the metal, plastic deformation will occur. Thirdly, at high impact energies, full scale plastic deformation is said to occur. Finally, rebound occurs when the elastic energy in the indenter and the bulk material of the test specimen is released.

3.6.2. Shore Scleroscope Tester

The Scleroscope test [Shore, 1918] is performed by dropping a diamond tipped hammer onto the test metal and then the height of hammer rebound is measured. It is therefore essentially a dynamic indentation test.

A glass tube holds the diamond tipped hammer and serves as a guide for it when it falls. The hammer is raised to the top of the tube by air suction and held by a catch. On release, no initial velocity is imparted on the hammer. The glass tube is graduated into 140 arbitrary equal parts, and the maximum height of rebound is measured on this scale.

3.6.3. The Developed Dynamic Tester

The tester developed uses a similar principle. The tungsten carbide indenter is dropped within a bearing guide. The time from first contact with the specimen to a second contact is measured. Newton's laws may be used to calculate the rebound height. This eliminates the error introduced by eye measurement of the rebound height.

3.6.4. Comparison of Static and Dynamic Hardness

Tests were carried out to establish a relationship between static and dynamic hardness [Tabor, 1951]. Two main points were discovered. First, the dynamic yield pressure P_d was always greater than the static yield pressure P_s. Secondly, the dynamic yield pressure is higher at greater velocities of impact. This is due to the fact that part of the energy required to produce an indentation is used in the viscous displacement of the metal around the indentation.

3.6.5. Meaning of Dynamic Hardness

As with static hardness, dynamic hardness is a measure of the yield limit of the material. If the rebound method is used to calculate the dynamic hardness, the effects of the viscous flow around the indentation are largely eliminated. The experiments carried out on dynamic hardness show that very light loads are needed to cause plastic deformation. Thus any loads applied in static tests must be applied slowly and smoothly.

4. SIGNIFICANCE OF INDENTER GEOMETRY

The theory of rigid perfectly plastic solids predicts indentation pressures, using conical indenters, which depend only on the indenter geometry and the yield stress of the material. With blunt cones, or with materials of a low ratio of Young's modulus E, to yield stress Y, the material displaced by the indenter is accommodated by an approximately radial expansion of the surrounding material. The indentation pressure then falls below the perfectly plastic value. indentation pressure for the cone is shown to correlate with the single parameter $(E/Y)\tan\beta$ where β is the angle of inclination of the indenter to the surface at the edge of the indentation.

4.1. Overview

Although the hardness test is an easy one to perform, its interpretation in terms of the stress - strain relation of the material is not straight forward due to the complex strain field produced by the indentation process. For ductile materials [Tabor, 1951] has shown that the mean contact pressure p_m can be related to the yield stress of the material Y, by an expression based on the theory of indentation of a rigid perfectly plastic solid, namely,

$$p_m = CY \tag{4.1}$$

Where C is a constant whose value is approximately 3, depending on the indenter geometry. However, if the material is highly elastic, the indentation pressures are lower than would be expected from equation (4.1). In such instances, the plastic and elastic strains in the region around the indenter are of comparable magnitude and hence the elastic deformation cannot be ignored.

The theoretical pressure [Hill, 1950] necessary to expand a spherical cavity from zero radius in an elastic perfectly - plastic solid is;

$$\frac{p}{Y} = 0.40 + \frac{2}{3}\ln(E/Y) \tag{4.2}$$

For blunt two dimensional wedges, and using relatively elastic materials the indentation pressure followed a relation of the form

$$\frac{p_m}{Y} = A + B \ln(E/Y) \tag{4.3}$$

Where A varies with the wedge angle and B is approximately constant (= 0.48) for wedges whose included angle exceeded 120°. One may compare this with the expression for a pressurized cylindrical expanding cavity from zero radius, namely;

$$\frac{p}{Y} = 0.26 + \frac{1}{\sqrt{3}} \ln (E/Y) \tag{4.4}$$

Also, by measuring the elastic recovery of the indentations, using a blunt wedge, the corresponding mean pressure is given by

$$p_m = \frac{E \cot \alpha}{2(1 - \nu^2)} = \frac{E \tan \beta}{2(1 - \nu^2)} \tag{4.5}$$

Where β is the angle of inclination of the wedge face to the surface of the solid ($\beta = \frac{1}{2}\pi - \alpha$) as in figure 4.1.

The angle β is a measure of the strain intensity associated with the deformation. One would expect the indentation pressure to be a function of both the wedge angle β and the material parameter E/Y. It is proposed that the indentation pressure induced by blunt indenters (small β) is governed by a single parameter $(E/Y) \tan \beta$. This parameter may be interpreted as the ratio of strain imposed by the indenter to the maximum strain which can be accommodated by the material before yielding.

4.2. Geometry of Deformation

The indentation produced by a rigid cone is shown in Figure 4.1a and that produced by a rigid sphere in Figure 4.1b.

$$\epsilon(x/a, y/a) \approx Kh/a = \tfrac{1}{2}Ka/R \qquad (4.8)$$

If the slope of the indentation at its edge is denoted by the angle β, then

$$\epsilon(x/a, y/a) \approx \tfrac{1}{2}K \sin\beta \approx \tfrac{1}{2}K \tan\beta \qquad (4.9)$$

for shallow indentations and small β.

This shows that the intensity of strain in a shallow indentation is approximately proportional to the slope of the indentation at the edge. In a conical indentation the strain is independent of the penetration. In an indentation of circular profile, the strain grows in direct proportion to the size of the indentation a.

4.3. Elastic Stresses

The stresses in an elastic semi-infinite solid which is indented by a rigid cone or sphere are known, provided the indenter is blunt and the strains remain small. These are summarized in table 4.1.

Table 4.1

Comparison of Stress Values
for
Conical and Spherical Indenters

	Cone	Sphere
Mean pressure p_m	$\frac{E \tan\beta}{2(1 - \nu^2)}$	$\frac{4E(a/R)}{3\pi(1 - \nu^2)}$
Maximum shear stress τ_1	p_m at (0,0)	$0.47\, p_m$ at (0,0.47a)
Mean principal stress σ	$2(1 - \nu)p/3 = \infty$ at (0,0)	$3(1 + \nu)p_m$ at (0,0)
Pressure for first yield $(p_m)_y$	$0.5\, Y$	$1.1\, Y$

The theoretically infinite pressure which occurs at the cone apex needs to be clarified. The stress at the apex is virtually hydrostatic and for an incompressible material ($\nu = ½$) it would be so. This means that the plastic flow caused by the high pressure at the apex is limited to a small region around the apex. Only when the mean pressure exceeds 0.5 Y for the cone, will appreciable plastic deformation begin. Even then, as with spherical indenters, the plastic region is confined to a small region beneath the indenter.

Another feature of the elastic stress system is that in each case there is a region of high hydrostatic pressure of approximately semicircular or hemispherical shape beneath the indenter. This pressure forces the surrounding material to expand radially to accommodate the material displaced by the penetration of the indenter.

4.4. Rigid Plastic Deformation

For materials such as those with a high value of E/Y, the theory of rigidly plastic solids has been successful in predicting the indentation pressure in terms of the yield stress of the material, except where the angle of indentation is shallow (β small).

Although the magnitude of the indentation pressure is correctly predicted, it is noticed that the mode of deformation obtained with a blunt indenter is different form the theoretical pattern. This is due to the fact that the deformation mode is affected by friction on the face of the indenter.

4.5. Elastic - Plastic Expansion of a Spherical Core

Between the point of first yield and the fully plastic flow, there is a range of behaviour where both elastic and plastic strains influence the deformation and the indentation pressure. An exact analysis of this condition is difficult in view of the changing shape of the elastic plastic boundary.

The process of a cone indentation is idealized by the elastic-plastic expansion of a cylindrical cavity. This approach led to a relationship between the

pressure within the cavity and the material parameter E/Y. This does not include the influence of the cone angle α, but may be extended to include this parameter by matching the volumetric expansion of the cavity to the material displaced by the indenter.

One may think of the indenter being encased in a hemispherical core of radius a. Within the core there is assumed to be a hydrostatic pressure p. Outside the core, the stresses and displacements are assumed to have radial symmetry. They are also assumed to be the same as in an infinite elastic perfectly plastic body which contains a spherical cavity under pressure. The elastic-plastic boundary lies at a radius c where $c > a$.

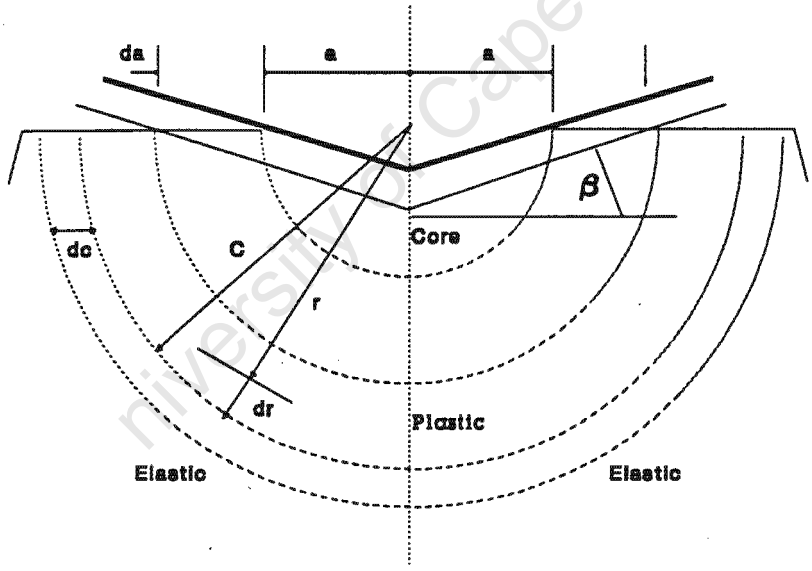

Figure 4.2 Idealized Model of an Indentation

At the interface between the core and the elastic-plastic boundary, two conditions must be satisfied: first, the radial displacement of particles lying on the boundary during an increment of penetration dh must accommodate the volume of material displaced by the indenter; and secondly, the hydrostatic pressure in the core must equal the radial component of stress in the external zone at $r = a$.

4.5.1. Conical Indentations

Here we take Figure 4.2 to represent the axisymmetrical indentation produced by a rigid cone. The stresses and displacements in the elastic-plastic region outside the core are taken from [Johnson 1970], and the pressure in the core is given by

$$\frac{p}{Y} = - \left[\frac{\sigma_r}{Y} \right]_{r = a} = \frac{2}{3} + 2 \ln (c/a) \qquad (4.10)$$

The conservation of the volume of the cone gives,

$$2\pi a^2 du(a) = \pi a^2 dh = \pi a^2 \tan \beta \, da \qquad (4.11)$$

Whereby the elastic - plastic boundary is given by,

$$\frac{E}{Y} \tan \beta = 6(1 - \nu)(c/a)^3 - 4(1 - 2\nu) \qquad (4.12)$$

Taking $\nu = ½$ (for an incompressible material) and substituting into (4.10) gives,

$$\frac{p}{Y} = \frac{2}{3} \left[1 + \ln \left[\frac{1}{3} \frac{E}{Y} \tan \beta \right] \right] \qquad (4.13)$$

The elastic - plastic boundary in the model coincides with the boundary of the core ($c/a = 1$) at $p_m/Y = 1.1$, and (4.13) is invalid below this pressure. At fully plastic pressure, $p_m / Y \approx 3$, the elastic - plastic boundary moves out to make $c/a \approx 2.5$. Observations [Johnson, 1970] suggest that the plastic region in metals extends radially for a slightly greater distance than this, but strain hardening shown by most metals will cause the boundary of first yield to extend further into the solid than the perfectly plastic theory would predict.

4.6. Conclusions

It has been show that the hardness of an elastic-plastic material to penetration by a blunt indenter is governed by a single parameter $(E/Y)\tan\beta$, where β is the inclination of the face of the indenter to the surface of the material, E is the elastic modulus of the material and Y its yield stress in compression. For spherical indenters, β is the angle of inclination of the indentation at its edges.

For values of $(E/Y)\tan\beta$ less than 2 the deformation is essentially entirely elastic and the mean pressure is given by the elastic equations although surface roughness may lead to some reduction in the mean contact pressure to below the expected value.

Plastic deformation begins in a small region contained below the center of the indenter at a pressure $\approx Y$ and spread with increasing values of $(E/Y)\tan\beta$. With spherical indenters, the spread is brought about by an increase in load. During this phase, the displacement of material is approximately radial from the point of first contact. The material displaced by the indenter is accommodated by the elastic-plastic expansion of the surrounding material. When the value of $(E/Y)\tan\beta$ reaches about 50 in the three dimensional case, the pressure has increased to approximately 2.8 Y which is sufficient to cause a change in the mode of deformation. The material displaced by the indenter is now free to pile up at the sides without any further increase in pressure.

When the transition between perfectly plastic and fully elastic behavior takes place, the mode of deformation is one of radial expansion which is caused by hydrostatic stress beneath the indenter. A model of the process may be found using the stress field generated due to the expansion of a spherical cavity in an elastic-plastic solid. If one adjusts the model so that there is a compatibility between the volume of the displaced material and the radial expansion in a semicircular region beneath the indenter, the predicted pressure and the measured contact pressure are in good correlation.

Significance of Indenter Geometry

Although the dependence on the single parameter $(E/Y)\tan\beta$ is theoretically restricted to small strains, and thus small values of β, it appears to correlate well up to angles of $\beta = 30°$. With sharper indenters, the mode of deformation is different and the correlation of indentation pressure to $(E/Y)\tan\beta$ is no longer appropriate.

5. DYNAMIC HARDNESS

The dynamic hardness may be defined as local resistance of a metal to indentation produced by a rapidly moving indenter. The most practical method is to allow the indenter to drop under the effect of gravity. It has been shown [Martell, 1895] that the volume of indentation so formed is directly proportional to the kinetic energy of the indenter. This implies that the metal offers an average pressure of resistance to the indenter and this can be expressed as the ratio

$$\frac{\text{energy of indenter}}{\text{volume of indentation}}$$

Suppose that the indenter is of spherical or conical form and that there is a constant pressure P resisting the impact. Also, assume that the projected area of the indentation at any time is A, then the force exerted by the metal on the indenter is $P A$. If the indenter then moves a further distance dx into the metal, then the work done is $P A\, dx$. The total work done in forming the indentation is then

$$\int P A\, dx = P V$$

where V is the volume of indentation. According to Martell, this may be equated to the energy of impact so that

$$P = \frac{\text{energy of impact}}{V}$$

This has the dimensions of pressure and is referred to as dynamic hardness. It has been suggested that the rebound energy should be taken into account when calculating the dynamic hardness.

It follows that the energy required to produce the indentation is equal to the energy of impact minus the energy of rebound. This is equal to the product of P and the volume of the remaining indentation. There may be an appreciable change of volume of the indentation (due to elastic recovery) when rebound occurs. This, as well as the energy of rebound, must be taken into account when calculating dynamic

hardness. If the height of rebound is used as a direct measure of dynamic hardness, it eliminates the problems of change of volume of the indentation due to elastic recovery [Shore, 1918].

5.1. Mean Dynamic Yield Pressure

The dynamic yield pressure P is assumed to be constant and not necessarily the same as the static pressure required to cause plastic flow. This, however, implies that when the pressure during impact reaches the value P, plastic flow occurs and as long as the plastic flow continues, the pressure remains constant. If after the impact, the volume of the remaining indentation is V_r, the work done as plastic energy in producing the indentation is

$$W_3 = P\,V_r \tag{5.1}$$

W_3 is the difference between the energy of impact W_1 and the energy of rebound W_2. One therefore needs to calculate W_2 and V_r.

Suppose that the indenter has a mass m and a spherical tip of radius r_1. Also, assume that it falls from an initial height h_1 and rebounds to a height h_2. After the collision it leaves a permanent indentation in the metal surface of chordal diameter $d = 2a$ (Figure 5.1).

The mechanisms involved in the dynamic indentations are assumed to be the same as those under static conditions. In other words, when the plastic deformation has been completed, there is a release of elastic stresses in the indenter and the indentation. The energy involved in the release of these stresses is equal to the energy of rebound of the indenter.

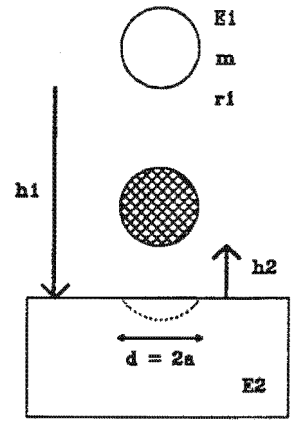

Figure 5.1 Schematic of the Indentation Process

After the impact, there is a release of elastic stress of the indentation and its radius of curvature will not be r_1, but somewhat greater, r_2. If one were to apply a suitable load F to the indenter for a short interval, it would deform the indentation elastically and according to Hertz's equation [Hertz, 1881] (see also Timoshenko and Goodier, 1970) it would just touch over the diameter $d = 2a$ so that

$$d = 2a = \left[\frac{6 F r_1 r_2}{r_2 - r_1} f(E) \right]^{1/3} \qquad (5.2)$$

Where:

$f(E) = (1 - \nu_1^2)/E_1 + (1 - \nu_2^2)/E_2$
E_1 and E_2 = Young's moduli of indenter and surface respectively.
ν_1 and ν_2 = Poisson's ratios of indenter and surface respectively.

As the indenter strikes the surface the force increases from zero to a final value F from equation (5.2) as the full contact across the diameter $d = 2a$ is

completed. At any instant when the contact diameter is 2 δ (where $\delta < a$) the force Φ on the indenter is given by

$$\Phi = F\frac{\delta^3}{a^3} \tag{5.3}$$

At this stage, due to the elastic deformation of both the indenter and the surface, the center of the indenter has descended a distance z

$$z = \frac{3\,\Phi}{4\,\delta} f(E) \tag{5.4}$$

Where $f(E)$ is the same as in equation (5.2).

Then the integral of $\Phi\, dz$ over the range $\delta = 0$ to $\delta = a$ is the total elastic energy stored in the surfaces K

$$K = \int_0^a \frac{3\,F^2}{2\,a^6} f(E)\,\delta^4\, d\delta$$

$$= \frac{3\,F^2}{10\,a} f(E) \tag{5.5}$$

This process is the exact converse of what happens when the surfaces recover elastically and the indenter is ejected from the indentation. But since the process is elastic, the energy involved in both cases is the same, so that K is equal to the energy of rebound.

$$W_2 = mgh_2 = \frac{3\,F^2}{10\,a} f(E) \tag{5.6}$$

The volume V_r of the permanent deformation left in the surface may be written as $V_r = (\pi a^4)/(4r_2)$. And thus:

$$W_3 = W_1 - W_2 = P V_r = P \frac{\pi a^4}{4 r_2} \qquad (5.7)$$

One may now express r_2 in terms of r_1 and F from equation (5.2)

$$\frac{1}{r_2} = \frac{1}{r_1} - \frac{3F}{4a^3} f(E)$$

$$W_3 = P \frac{\pi a^4}{4 r_1} - \frac{3F^2}{16a} f(E) \qquad (5.8)$$

The force at F at the end of the indentation is equal to $P \pi a^2$. The first term of equation (5.8) is $P V_a$ where V_a is the *apparent* volume of the indentation which would be obtained if the indentation were to have the same radius of curvature as the indenter (r_1). The apparent volume would thus be $V_a = (\pi a^4 / 4r_1)$. The second term of the equation by comparison to equation (5.6) is equal to $^5/_8 W_2$ and thus

$$W_3 = P V_a - {}^5/_8 W_2 \qquad (5.9)$$

$$P = \frac{mg(h_1 - {}^3/_8 h_2)}{V_a} \qquad (5.10)$$

The validity of this analysis depends on the assumption that the internal forces occurring in the actual impact are exactly the same as those in the analytical model just derived. In particular, the elastic waves set up in the indenter and the specimen are assumed to absorb a negligible amount of energy [Tabor, 1951].

5.2. Effect of Variation of Yield Pressure

The above derivation assumes that P is constant throughout the impact process. There are two reasons, however, why P may be expected to vary during the collision. The first is a dynamic effect associated with the kinetic displacement of the metal during impact. This will tend to increase the value of P during the initial stages of impact when the velocity of displacement is at a maximum. The second reason is that work-hardening of

the material will occur during the formation of the indentation. As a result, P will increase during the impact in a similar manner to that observed with static hardness measurements (Compare with Brinell hardness). If one thus assumes an analogy with static hardness, one may write

$$P = k\,d^{\,n-2} \tag{5.11}$$

where n lies between 2 and 2.5. The work W_3 done in expanding a volume V_r becomes

$$W_3 = \frac{4}{n+2}\,P\,V_r \tag{5.12}$$

where P is now the mean pressure at the end of the deformation process. This is also the pressure involved in calculating the rebound. If one now substitutes this value of W_3 into the appropriate equations, the mean pressure at the end of the indentation process becomes,

$$P = \frac{n+2}{4}\;\frac{mg\left[\,h_1 - \dfrac{2n-1}{2(n+2)}\,h_2\,\right]}{V_a} \tag{5.10a}$$

The last term in the bracket varies from $^3/_8\,h_2$ to $^4/_9\,h_2$ as n varies from 2 to 2.5, so that this term gives lower values for P. The term in front of the main bracket increases from 1 to 1.12 as n increases from 2 to 2.5. The overall effect is that it gives slightly higher values of P than equation (5.10), but the difference is never greater than 10 %.

If one notes that at the end of the indentation process, $F = \pi\,a^2\,P$ and one assumes a value of 0.3 for the Poisson's ratio of both the indenter and the metal, then

$$h_2 = \frac{2.7\,a^3\,P^2}{mg}\left[\frac{1}{E_1} + \frac{1}{E_2}\right] \tag{5.6a}$$

Since the apparent volume of indentation V_a is proportional to a^4, this means that h_2 is proportional to $V_a^{3/4}$ for any fixed material. If one thus plots h_2 against V_a on logarithmic coordinates, one should obtain straight lines with a slope of $^3/_4$, if P is constant. The following results were taken from Edwards and Austin (1923).

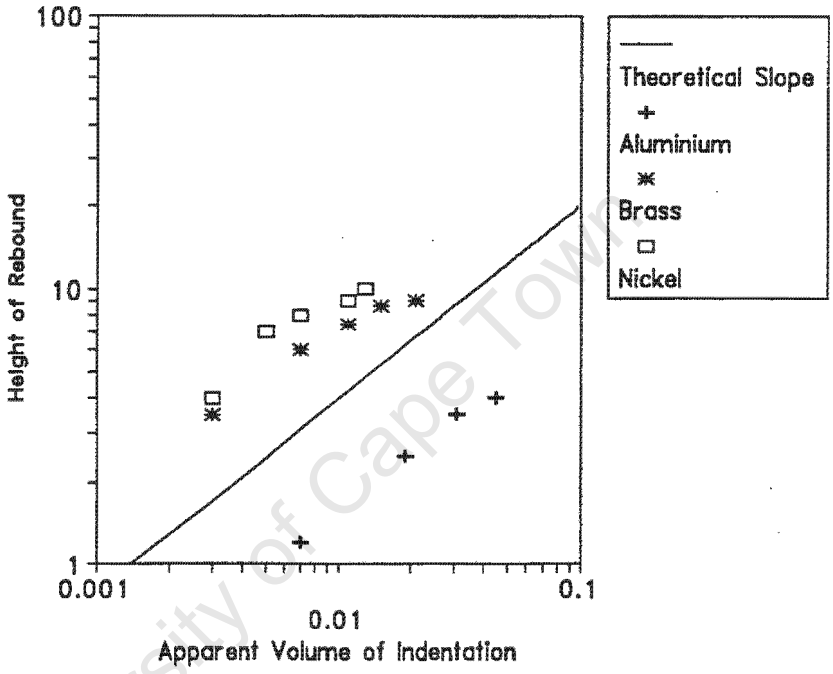

Figure 5.2 Rebound Height versus Apparent Volume of Indentation

If P is not constant and varies as given by equation (5.13), then the logarithmic graph of h_2 against V_a is still a straight line, but, the slope has a value of $(2n - 1)/4$. This means that it varies from $^3/_4$ to 1 as n varies from 2 to 2.5.

Also, for indentations of a fixed diameter, h_2 should be proportional to

$$P^2 \left[\frac{1}{E_1} + \frac{1}{E_2} \right]$$

If one therefore, plots h_2 against

$$P \left[\frac{1}{E_1} + \frac{1}{E_2} \right]^{1/2}$$

on logarithmic ordinates, one should obtain a straight line of slope $^1/_2$. Results taken from the same paper are plotted in figure 5.3.

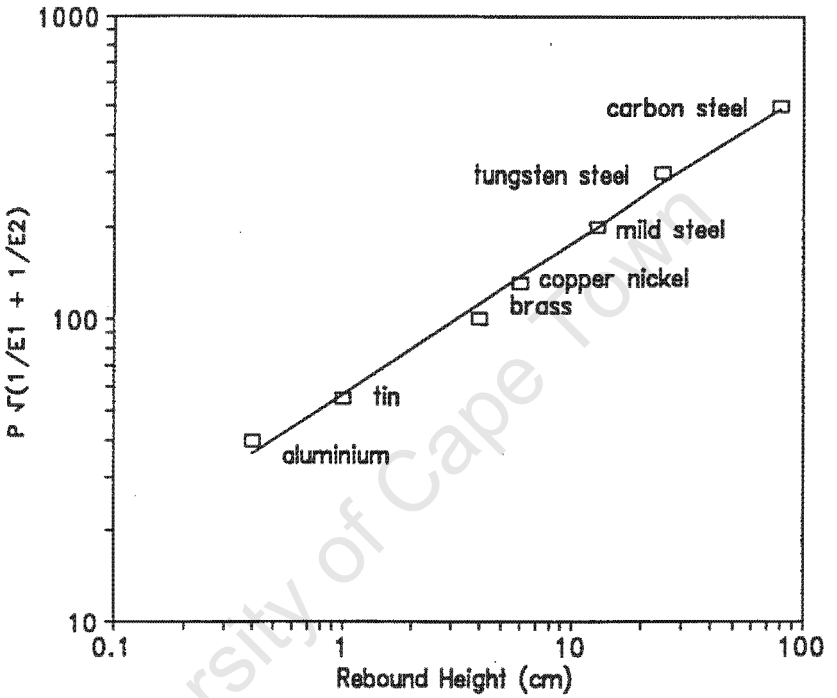

Figure 5.3 $P\,(^1/E_1 + {}^1/E_2)^{1/2}$ versus Rebound Height

If one now eliminates a from equation 5.10 and one calculates a resulting relationship between h_1 and h_2 and P the following formula is obtained

$$P^5 = \frac{{h_2}^4}{(h_1 - {}^3/_8 h_2)^3} \quad \frac{m\,g}{{r_1}^3} \quad \frac{10^4}{\pi^5\, 4^3\, 3^4} \left[\frac{1}{f(E)} \right]^4 \qquad (5.13)$$

When $\nu_1 = \nu_2 = 0.3$, then equation 5.13 becomes

$$P^5 = \frac{{h_2}^4}{(h_1 - {}^3/_8 h_2)^3} \quad \frac{m\,g}{109\,{r_1}^3} \quad \frac{1}{(^1/E_1 + {}^1/E_2)^4} \qquad (5.14)$$

Since the term involving Young's moduli does not vary much for most metals, one may treat this factor as constant and plot P as a function of h_2

and height of fall h_1. The theoretical curve for a given indenter is shown in figure 5.4.

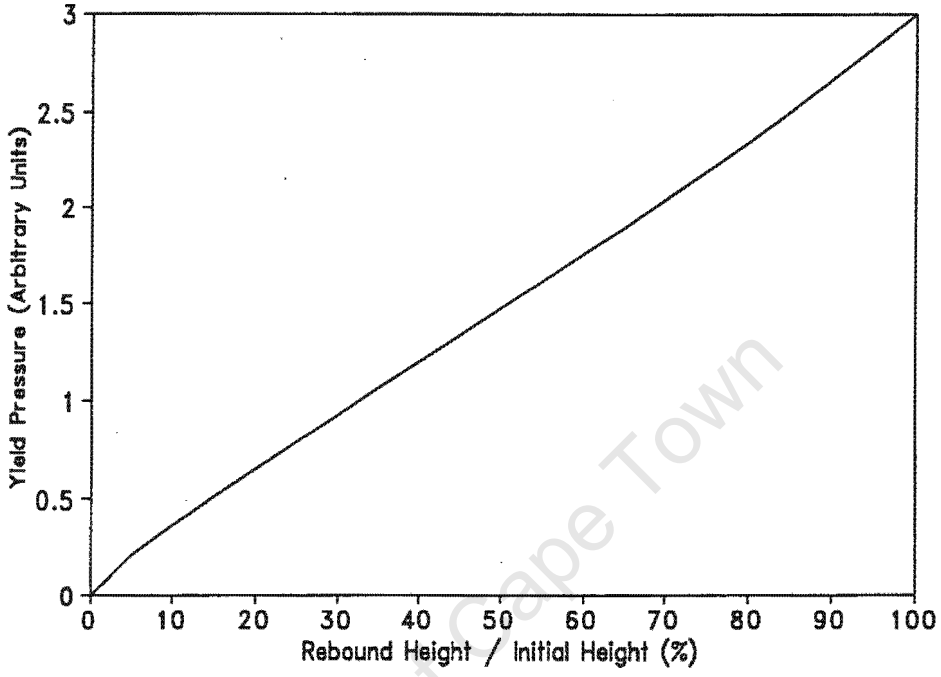

Figure 5.4 Dynamic Yield Pressure as a function of Rebound Height

It is, however clear that even if the metal does not work-harden, and even if the velocity of impact has no effect on P, the dynamic yield pressure given in Figure 5.4 [Tabor, 1951] will not be a single valued constant of the metal. It will depend on the size of the indentation formed, corresponding to the transition from the onset of plastic deformation to fully plasticity. Thus with light impact, where the collision may be almost entirely elastic, the pressure P involved will only be $^1/_{2.5}$ times the pressure involved in a heavier impact. This has been observed in some impact experiments described by Davis (1949). With a steel ball of diameter 1 cm falling on to a tool steel surface, the onset of plastic deformation occurred for a height of fall of 1 cm and a corresponding yield pressure P of about 160 kg/mm^2.

It is evident, therefore, that Figure 5.4 is approximately valid, if the vertical axis refers to the yield pressure during the collision itself. If by yield pressure one means the pressure associated with full plastic deformation the results in Figure 5.4 will be valid for the smaller heights of rebound since

here the impressions will be fairly large. It will not be valid for the greater heights of rebound since here the collision process approaches the conditions associated with the onset of plastic deformation. In this region, as can be seen, the yield pressure associated with full plasticity will be two to three times larger. Thus if we wish to plot yield pressure as a function of the height of rebound (for a fixed height of fall) at the fully plastic stage, the lower portion of the curve will be similar to that shown in Figure 5.4, whilst the upper portion will be pushed over to the left. This will introduce a more marked S-shaped curve.

5.3. Elastic Collisions

An interesting situation occurs when the height of rebound equals the height of fall. In this case, the processes of impact and rebound become entirely elastic. If one goes back to the Hertzian equation and calculates the final average pressure P_e developed between the indenter and the anvil in an elastic collision, one obtains the relationship

$$P_e^{\,5} = \frac{8^3\ 10^4\ mgh_1}{5^3\ \pi^5\ 4^3\ 3^4\ r_1^{\,3}}\ f(E)^{-4} \qquad (5.15)$$

Equation (5.15) obtains the same value for P as does equation (5.14) when h_2 is put equal to h_1. One may draw two conclusions from this result. Firstly, equation (5.14) is valid right up to 100 percent rebound. In the latter equation, the pressure obtained is the final mean pressure between the indenter and the specimen. Secondly, plastic deformation will not occur if the yield pressure of the specimen is higher than the value of P_e given in equation (5.15). If it is less than P_e, plastic deformation occurs and the value of P in equation (5.14) gives the dynamic yield pressure of the material.

It is evident that the rebound method of dynamic hardness testing will not discriminate between materials having a yield stress above P_e since they would give a rebound of 100 percent. In practice, 100 percent rebound is not attainable due to energies lost due to friction and dissipation of elastic waves. To increase the range of the apparatus, the experimental conditions

may be modified to give a higher value of P_e in equation (5.15) This may be achieved by increasing the mass of the indenter or by increasing the height of fall. If one increased either of these by a factor of 32, the value of P_e would double. A more sensitive method would be to decrease the radius of the tip of the indenter. A decrease of r by a factor of 3.2 will double the value of P_e.

5.4. Comparison of Dynamic and Static Hardness

It is interesting to compare the static and dynamic hardness of metals. One may consider impact experiments [Tabor, 1951] carried out on massive anvils using hard steel balls on various metals. The dynamic yield pressure P_d was calculated by measuring h_1, h_2 and the chordal diameter d. Equation (5.10) was used. Static experiments were also carried out to determine the static yield pressure P_s required to produce indentations of similar diameter. The results showed two main points. Firstly, the dynamic yield pressure P_d was always greater than the static yield pressure P_s. This difference was particularly marked with soft metals. Secondly, the dynamic yield pressure is higher at greater velocities of impact. This suggests that calculating the dynamic yield pressure from equation (5.10), ie. from the energy required to produce a indentation of a given volume, part of the energy is used in the viscous displacement of the metal around the indenter.

5.5. Meaning of Dynamic Hardness

Dynamic hardness is the pressure with which a metal resists local indentation by a rapidly moving indenter. If the speed of impact is not excessive, the dynamic yield pressure is of the same order of magnitude as the static yield pressure. As with static hardness, dynamic hardness is essentially a measure of the elastic limit or yield stress of the metal. The actual value of the yield pressure depends not only on the size of the indentation, but also on the velocity of impact and the way in which it is calculated. If the dynamic yield pressure P_d is calculated from the energy required to give an indentation of certain volume, it is larger than the static yield pressure P_s and increases with velocity of impact. This is particularly noted with soft metals and it seems that since large volumes of metal are displaced,

appreciable forces are required to produce the 'viscous' flow of the deformed metal around the indentation. This view is confirmed if one calculates the yield pressure from the height of rebound. To do this one need only rearrange equation 5.6a. The suffix r may be added to the P to indicate that it is calculated from rebound height.

If the dynamic hardness is calculated from the height of rebound, the effects of the viscous flow are largely eliminated. At the end of the impact, all plastic flow has ceased and no further bulk displacement of the metal around the indentation occurs. The deformation around the indenter essentially elastic and any kinetic energy imparted on the indentation is reversible. Thus the pressures involved in this part of the collision P_r are only slightly higher than those involved in similar indentations under static conditions.

This conclusion shows that the large values of P_d cannot be due to work-hardening which may occur rapidly during the formation of the indentation. For at the end of the impact where the work-hardening would be at a maximum, the effective yield pressure P_r is much smaller than the mean dynamic yield pressure P_d which is involved during the course of the impact itself.

Thus dynamic hardness values obtained from rebound measurements will yield values which are close to those obtained in static measurements. Values obtained from the ratio of energy to the volume of the indentation will also be of the same order as the static values. With hard metals, the difference will be of the order of a few percent, but with soft metals, the difference is more marked, and will increase with the velocity of impact.

Another conclusion may be drawn from this work and applied to static work. Dynamic experiments show that very light impacts are required to produce plastic flow of metals. Thus, any impact during the process of static hardness experiments will lead to a hardness value which is lower than the true value. Static experiments must thus be carried out very smoothly.

6. ELASTIC RECOVERY OF CONICAL INDENTATIONS

In the previous chapter it was shown that the elastic energy released when a spherical indenter strikes an elastic - plastic material could account quantitavely for the observed rebound. This chapter describes a similar investigation using conical indenters.

6.1. Elastic Recovery

A number of assumptions must be made in order to simplify the calculations. Firstly, the recovered indentation is a right circular cone and that the free surface of the specimen is flat. Secondly, the resulting contour is also conical with the same semi - angle as that of the cone.

6.2. Dynamic Indentation and Elastic Recovery

When a conical indenter strikes a metal surface with energy U_1 it performs both elastic and plastic work on the metal specimen until all the energy is transferred. Elastic recovery occurs and the indenter rebounds with energy U_2. If the elastic processes are the same as those which occur under static loads, one may calculate U_2 from the elastic constants of the material.

6.3. Energy involved during Elastic Recovery

First, for simplicity, one may assume the indenter to be perfectly rigid. Secondly, the mean pressure throughout the indentation process is assumed to be constant, although it need not be the same as that under static conditions. The total elastic recovery of the indentation is

$$\Re = \frac{\pi}{2} y = \pi pa \left[\frac{1 - \nu^2}{E_1} \right] \qquad (6.1)$$

E_1 = Young's Modulus of specimen
ν_1 = Poisson's Ratio of specimen

2a = diameter of permanent indentation formed (Figure 6.1)

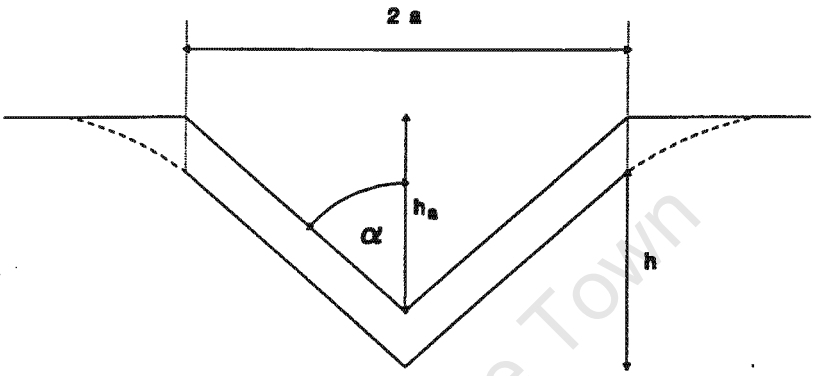

Figure 6.1 Diagram of Conical Indentation

The elastic work released by the indentation as it recovers is

$$U_2 = \int p\pi a^2 d\Re = \int_0^a p\pi a^2 \cdot \pi p \left[\frac{1 - \nu^2}{E_1} \right] da = p \frac{\pi a^2}{3} \Re \qquad (6.2)$$

Also, the plastic work done on the specimen is

$$U_1 - U_2 = p * (\text{volume of recovered indentation}) \qquad (6.3)$$

The height of the initial indentation is (Figure 6.1)

$$h = a \cot \alpha \qquad (6.4)$$

The decrease in height due to the elastic recovery is

$$y = \frac{2}{\pi} \Re \tag{6.5}$$

The height of the recovered indentation is then

$$h_a = h - y = h - \frac{2}{\pi} \Re \tag{6.6}$$

and the volume of the permanent indentation left after the elastic recovery is $\pi a^2/3$ times this. Also from equation (6.3) we have

$$U_1 - U_2 = p \frac{\pi a^2}{3} \left[h - \frac{2}{\pi} \Re \right] \tag{6.7}$$

Combining this with equation (6.2) gives

$$U_1 - U_2 \left[1 - \frac{2}{\pi} \right] = p * (\text{nominal volume of indentation}). \tag{6.8}$$

Nominal volume of indentation = an indentation of the same geometric shape as the conical indenter.

A careful consideration shows that if the indenter also deforms elastically, an identical result is obtained, although here, U_2 includes the rebound energy due to the elastic recovery of the indenter. As a general equation one thus has

$$\text{Impact energy} - 0.363(\text{rebound energy}) = p * (\text{nominal volume of indentation}). \tag{6.9}$$

The analysis of impact of by spherical indenter [Tabor, 1951] shows a similar relationship, except that the numerical coefficient of U_2 is $^3/_8$ instead of 0.363.

6.4. Ratio of Rebound to Impact Energy

In an impact experiment, the simplest quantity to measure is the energy of impact U_1 and, U_2 the energy of rebound. From equation (6.8) the relationship between impact and rebound energy is

$$U_1 = p\,\frac{\pi a^2}{3}\,h + \left[\,1 - \frac{2}{\pi}\right] U_2 \qquad (6.10)$$

The rebound energy is obtained from equation (6.2) and is equal to $\pi p a^2 \Re/3$ and thus

$$\frac{U_1}{U_2} = \frac{h}{\Re} + \left[\,1 - \frac{2}{\pi}\right] = 0.363 + \frac{h}{\Re} \qquad (6.11)$$

If one includes the elastic recovery of the indenter as well as the indentation and taking note of equation (6.4), one obtains the following

$$\frac{U_2}{U_1} = \pi\, p \tan\alpha \left[\frac{1 - \nu_1^2}{E_1} + \frac{1 - \nu_2^2}{E_2}\right] \qquad (6.12)$$

For steels, assuming $\nu_1 = \nu_2 = 0.3$, then

$$\frac{U_2}{U_1} = 2.85\, p \tan\alpha \left[\frac{1}{E_1} + \frac{1}{E_2}\right] \qquad (6.13)$$

One may deduce that the ratio of energies is equal to the ratio of height of fall to height of rebound, and hence equation 6.13 becomes:

$$\frac{h_2}{h_1} = 2.85 \text{ p} \tan \alpha \left[\frac{1}{E_1} + \frac{1}{E_2} \right] \qquad (6.14)$$

As in the case of the sphere, the value of the dynamic yield pressures are generally a little higher than the static values [Stilwell & Tabor, 1961]. Also, the ratio of h_2 / h_1 is more or less independent of h_1 as one would expect from equation 6.14.

7. DESIGN OF INDENTER AND RESULTS

The design of the dynamic hardness tester was based on the Scleroscope [Shore, 1918]. The hardness test is essentially a dynamic indentation test wherein the indenter is dropped from a fixed height onto the surface of the material being tested. The height of rebound is then a measure of the hardness of the material. Two types of indenters were used in this investigation. One was a spherically tipped indenter, while the other was conically tipped indenter. The results of both are discussed and compared.

The indications obtained by the use of this instrument depend on the resilience of the indenter as well as that of the material being tested. By resilience is meant the return to original form after elastic compression. Since both the indenter and specimen deform elastically, both must be taken into account as this is essentially what causes the rebound of the indenter. The permanent deformation of the test material is also an important factor. When the indenter falls onto a soft surface, it penetrates that surface to some extent before rebounding and produces a minute indentation. In doing so, part of the energy of fall is absorbed and the energy available for rebound is comparatively small. If the indenter is dropped onto a hard surface, the size of the indentation is much smaller, so that less energy is absorbed in making it. The rebound of the indenter in this case is therefore much higher than before. The height of rebound rather than the volume, diameter or depth of indentation is taken as a measure of the hardness, as it is the most readily measured parameter.

7.1. Design of the Indenter

The tester consists of two separate units; the indenter and the electronic measuring device [Refer to appendix A for a photograph of the tester]. The indenter consists of two parts; the housing and the shaft [Refer to appendix E for the drawings of the indenter, housing and shaft]. The shaft is made of tungsten carbide and its tip is ground with a spherical or conical profile. Thus, the shaft of the indenter is raised and dropped onto the test specimen. The housing serves as a guide for the indenter and also contains the electronic pickup to measure the time of rebound. The base of the housing

has a rectangular profile to facilitate the location of the electronic pickups and also to provide stability.

The electronic unit contains a timing device to measure the time of rebound of the indenter. The unit also contains a programmable chip (EPROM) which enables the time of rebound to be converted to a hardness value. The chip is programmed with empirical data which has been gathered from calibration experiments. Thus, since there is sufficient memory in the chip to allow four separate ranges to be programmed, the four most common hardness ranges are used. In other words, the time of rebound is directly converted to Vickers, Brinell, Rockwell C and Rockwell B scales by the unit. These values may be directly accessed via a selection switch on the front panel of the tester. This means that the operator only need perform one test and can then obtain the hardness of the workpiece in any of the above mentioned scales. Since the values have been programmed empirically, the error involved in converting from one hardness scale to another is not encountered.

7.1.1. Specifications for the Tester

Although the specifications for the tester were originally based on similar tests found in the literature survey, many were later altered due to problems encountered in the experimental procedures.

The decision to measure time of rebound (and hence calculate the height) was made to keep the electronics as simple as possible, and also to keep the pickup mechanism simple, easy to maintain and replace. There are two sets of electronic pickups in the base of the indenter and these may be individually accessed by means of a selector switch on the side of the display unit. This is done so that if one is damaged, the other may be utilized until a repair is made.

The indenter is made of a single shaft of tungsten carbide. This has been done to avoid the problems of joining a tip to the shaft. Since the shaft may be readily removed, it is a simple procedure to dress the tip in the event of

damage. Also, the dressing of the tip does not involve the removal of a great deal of material, and thus the indenter may be used repeatedly.

Another advantage of using a single shaft, is that a different tip may be ground at either end of the shaft. The user may specify that both ends have an identical tip so that in the event of damage, the shaft may simply be reversed and used until it is convenient to repair the damage. Another possibility is that one may desire to have a spherical tip at one end and a conical tip at the other. This, together with a spare set of programmable chips, will enable the user to choose the type of test he wishes to employ.

7.2. Effect of Changing Design Parameters

A number of physical parameters may be altered to affect the results. These may also affect the life of the tip. Among these are, the tip dimensions r_1 or α, initial height h_1, or the mass m. Increasing the mass or initial height, increases the stress on the tip, as does reducing α or the radius. All these factors lead to a reduced tip life, and their advantages should be weighed against this consideration. The effects of these parameter changes on the resultant dynamic yield pressure are described in the sections below.

7.2.1. Effects on Spherical Indenters

As mentioned in chapter 5, to increase the range of the hardness test, one may increase the mass of the indenter m or the height of fall h_1. These two alterations are easily facilitated, but as can be seen from the formula below, the effect of these changes will be small. For example, in the case of 100 percent rebound when h_2 is equal to h_1 the value of the dynamic yield pressure P, will double if either m or h_1 is increased by a factor of 32. Also, this change will lead to higher stress being placed on the tip, especially with hard test materials, and hence, the life of the tip will be significantly reduced.

$$P^5 = \frac{h_2^4}{(h_1 - {}^3/_8 h_2)^3} \quad \frac{m\,g}{109\,r_1^3} \quad \frac{1}{({}^1/E_1 + {}^1/E_2)^4} \qquad (5.14)$$

A more sensitive way to increase the range is to decrease the radius of the tip. If one again takes the example of 100 percent rebound, it may be shown that a decrease of r_1 by a factor of 3.2 will double the value of P. The effect of changing the radius is shown in figure 7.1. Since the shaft of the indenter has a fixed radius, it is more difficult to change the tip radius than either of the other parameters. For this reason, the exact range of application must be known in order to optimize the design.

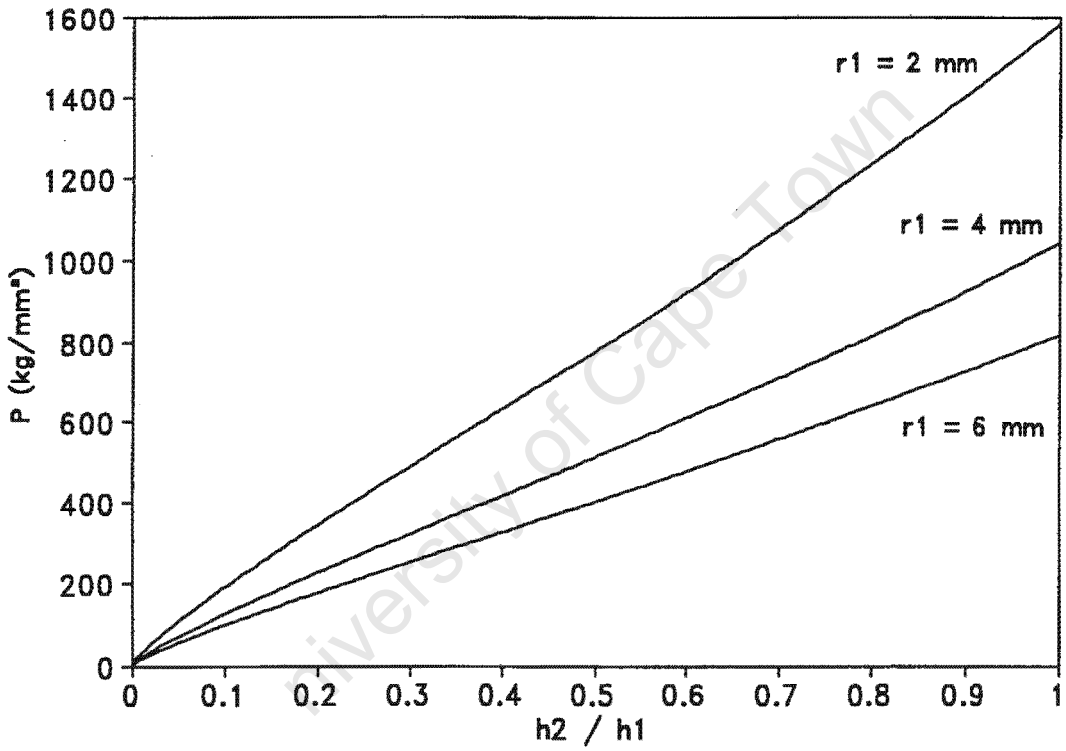

Fig 7.1 Effect of changing Tip Radius on Yield Pressure

7.2.2. Effects on Conical Indenters

Unlike with the spherical indenter, only two parameters affect the value of P. These are h_1 and α. From the following equation, it may be seen that changing h_1 will have little effect on P and thus changing α is the only viable alternative.

$$\frac{h_2}{h_1} = 2.85\ p \tan \alpha \left[\frac{1}{E_1} + \frac{1}{E_2} \right] \qquad (6.14)$$

The effect of altering α is shown in figure 7.2.

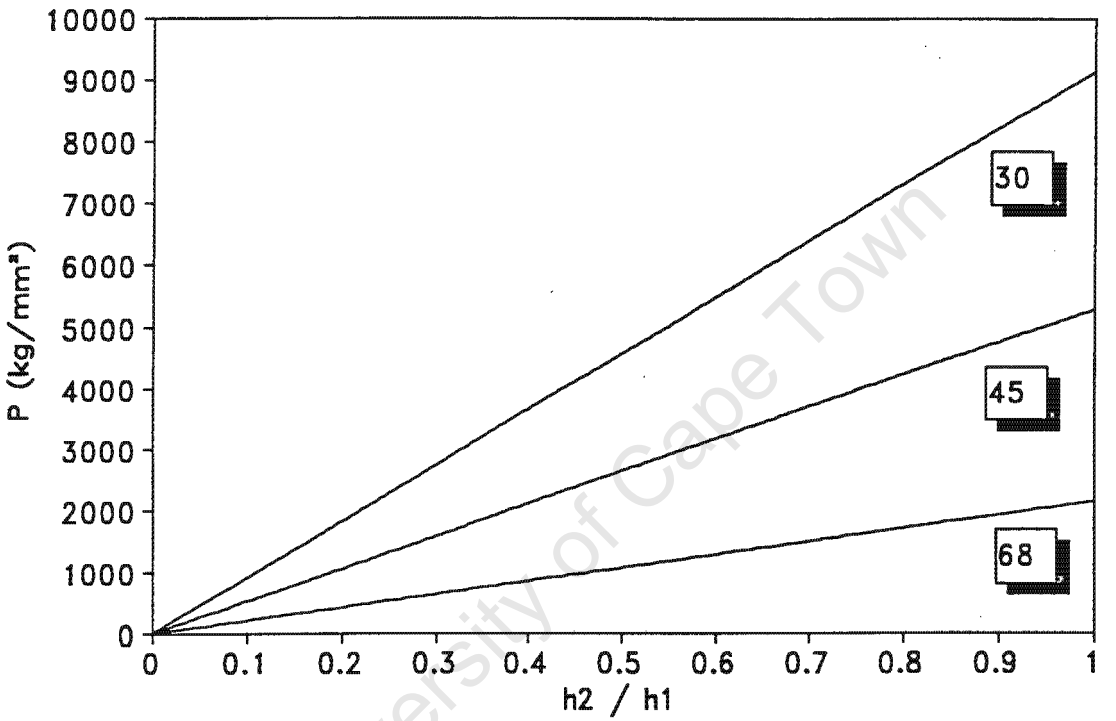

Fig 7.2 Effect of changing Cone Angle on Yield Pressure

In chapter 4 it was shown that the hardness depended on the parameter (E/Y) cot α. The theory, however only holds for $\alpha > 60°$. For this reason, an angle of $\alpha = 68°$ was chosen since it corresponds approximately to that of the Vickers indenter. Smaller angles were also tested, but due to brittle nature of tungsten carbide, the tip of the indenter became visibly damaged after a short period of time (approximately 100 indentation tests). The damage first became apparent when tests on the calibration blocks showed inconsistent results. Results from the calibration block would suddenly increase by two or three Rockwell points. Careful investigation of the indenter revealed that the cone had lost its tip. Instead of the tip having a

shiny surface like the parent material, it had a dull appearance. The damage is shown schematically in the diagram below.

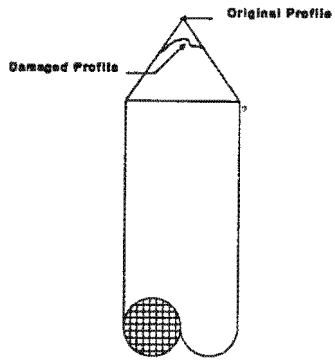

The extent of the damage was also related to the hardness of the test piece. This was expected, since harder material places more stress on the tip. For this reason, a maximum hardness for test materials is given at 65 Rc, since tests showed that even the chosen cone semi angle of 68° became damaged at repeated tests above this hardness.

7.2.3. Comparison of Indenters

The curves shown in figure 7.3 are the theoretical dynamic yield pressures obtained from the sphere (r_1 = 3.175 mm) and the cone (α = 68°). It is interesting to note that for a given value of yield pressure, the rebound height for a spherically ended indenter is about double that for a conical one. This indicates that the proportion of elastic work done during the indentation with the spherical indenter is greater than that with the conical tip. Much higher initial heights are thus needed to produce the same amount of plastic work as with the conical indenter. These higher energy requirements demand careful support of the specimen since energy dissipation may lead to inaccuracies.

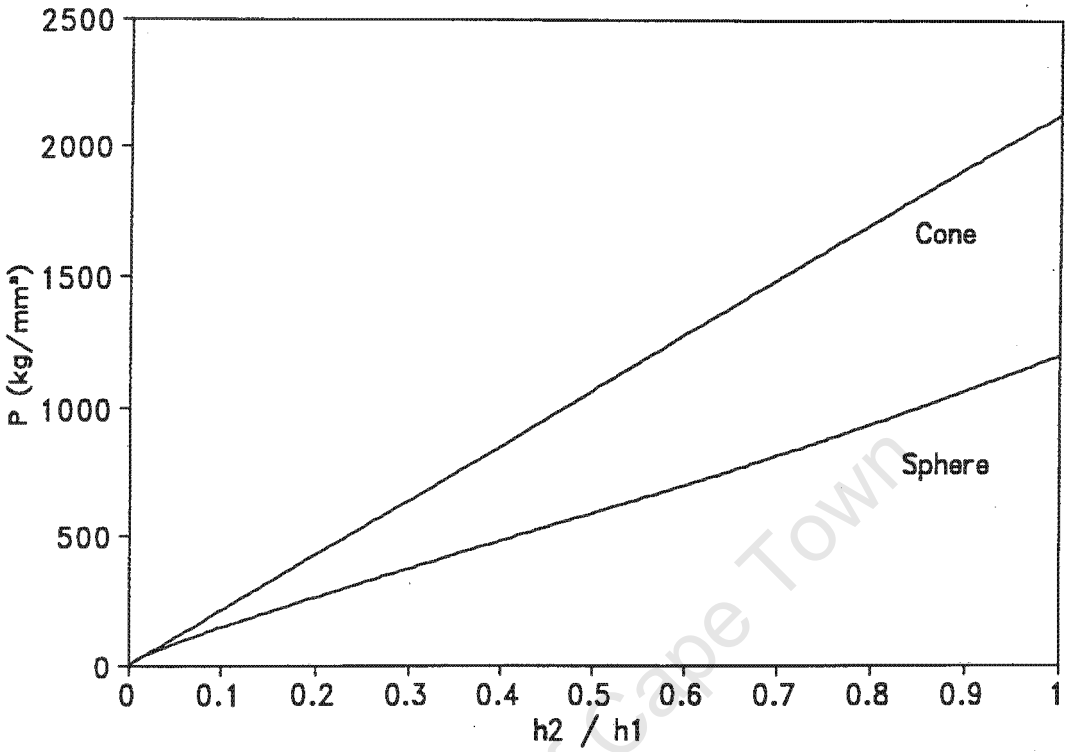

Fig 7.3 Comparison of Theoretical Dynamic Yield Pressure using the Cone and Sphere

7.3. Test Procedures

Although the tester is intended for use in the field as well as in the laboratory, this dissertation has only examined the validity of the theory and the viability of such a tester for use in a laboratory. Since the majority of the tests were carried out to calibrate the apparatus, strict test procedures were adhered to. These are described in the following paragraphs.

To perform a hardness test with the dynamic hardness tester, the tester should be placed on the workpiece in a near vertical position with the base of the tester in firm contact with the workpiece. The reset button on the tester must be pressed to prepare for the next test. At the same time, the selector switch may be used to access the desired hardness scale. Whilst the base and housing are held steady with one hand, the indenter is then raised to its upper position with the other. It is then held in this position and then simply

released and allowed to strike the surface of the workpiece. The hardness of the metal is then read directly off the display on the tester. After the test has been completed, the selector switch may be pressed in order to obtain the hardness in any of the other three programmed scales. To perform another test, the reset button is activated and the procedure repeated. Pressing the reset button does not clear the display, it merely resets the timer. After the second test has been performed, the previous display is overwritten with the new result.

To minimize errors, the hardness tester must be held in the near vertical position. To achieve this, the supplied support should be placed on a level surface and checked with a level to ensure that it is horizontal. The support is a solid rectangular piece of mild steel 60 mm x 60 mm x 250 mm with two opposite faces ground parallel. The opposite faces of the workpiece must also be parallel with each other. A small amount of grease should also be applied between the workpiece and the support in order to ensure good contact. Although this is not essential, it does increase the consistency of the results. It also prevents the specimen from moving on the base during the test and thus makes it easier to position the tester relative to the workpiece. This is useful in preventing two tests from being performed on the same spot.

The indentations should also be at least 1.0 mm apart and only one reading may be taken at the same spot. If a second test is performed on the same spot, or an old indentation is struck during a test, the measured hardness is considerably higher than that of the virgin material. Although it is difficult to quantify this error since it is more likely to strike the edge of a previous indentation than the center, the result of a test performed too close to an old indentation usually shows a result five or six Rockwell points higher than that of the parent metal. Flat workpieces with parallel surfaces may be tested within 6 mm of the edge when properly supported by the base support. Tests performed too close to the edge make a ringing sound and the results are so erratic that they proved futile to record. The calibration showed that tests performed within this designated region gave the best results.

Thin material should be securely clamped to absorb the inertia of the hammer. The sound of the impact is an indication of the effectiveness of the clamping [Tabor, 1951]. A dull thud indicates that the workpiece has been clamped correctly, whereas a ringing sound indicates a workpiece which has not been clamped correctly, is warped or is not properly supported. Five hardness determinations should be made and their average taken as representative of the hardness of the workpiece [Shore, 1918]. The number of tests was hoped to be reduced with the more modern measuring techniques, but it was felt that for the calibration procedure, this number should be used. Examples of the tests and statistical analysis are shown in appendix F. The standard deviation of the results where time is measured is in the region of one millisecond. Since the sensitivity of the apparatus is no greater than this, it was decided that larger sampling procedures were not required.

Once the tester had been programmed with the various hardness ranges, further tests were carried out on specimens to determine the number of tests required to achieve a result with an associated error comparable to that which is set by the static test procedures. The results of such a test may also be found in appendix F. The statistical analysis shows that a similar error is obtained using five or all ten results. If less than five tests are performed, the result may not fall within the required error limits and thus it is suggested that the number of tests remain at five.

7.4. Results

The experiments were carried out firstly to validate the correlations between the various common static hardness tests. This was done in order that an accurate relationship may be found between these hardness tests and the dynamic tests. Each specimen was tested on a Rockwell, Vickers and Brinell machine. The results from each of these tests was then programmed empirically into the EPROM to eliminate the error associated with converting from one hardness scale to another. It has also been stated that the dynamic yield pressure P_d is always higher than the static yield pressure P_s [Tabor, 1951]. Table 7.1 shows the comparison between these pressures. The table shows the specimens sorted in numerical ascending order

(according to the static yield pressure). A full description of the material types and properties together with the results from which the pressures were obtained may be found in appendices B through D. The dynamic pressures for the sphere and cone were obtained from equations 5.14 and 6.14 respectively. The values for the static pressure were derived from the Vickers hardness value of the material, where $P = H_v / 0.927$. This scale was used since it covers the entire range of the test specimens.

Table 7.1

Dynamic Yield Pressures for both cone and sphere of the calibration specimens

Specimen	P_{static} (kg/mm²)	P_{cone} (kg/mm²)	P_{sphere} (kg/mm²)
3 Alu	106	70	136
8	117	55	111
2	119	55	111
4 Brass	129	131	219
1 Alu	146	71	131
7 Steels	194	209	290
D	210	226	302
A	219	218	331
6	220	223	315
5	221	229	321
F	518	644	651
E	593	687	710
H	680	782	755
C	688	795	731
9	690	750	733
B	853	885	817
10	885	962	887
G	917	958	884

The results verify the fact that in the case of the sphere, the dynamic yield pressure is higher than the static yield pressure. If one takes experimental error into account, the ratio of P_d / P_s is approximately 1.2 for aluminium and 1.1 for steels.

In the case of the cone, however, it is interesting to note that the values for steels are approximately equal, whereas the value for aluminium is approximately ½.

If the rebound height is used to calculate the hardness, the effects of viscous flow around the indenter are eliminated. This means that the kinetic energy imparted on the indentation is predominantly reversible and one would expect the pressures to be equal.

The following conclusions may thus be drawn. Firstly, there is bulk displacement of the parent metal in soft materials such as aluminium. This would account for the fact that the values for the spherical indenter are higher than those of the conical one. Also, the conical dynamic tester gives a more accurate account of yield pressure of soft metals than does the static test. This may be deduced from the fact that even in the static tests, there was a considerable amount of pile - up around the indentations produced in soft metals. A similar observation was made for the spherical dynamic indenter. In the case of the conical dynamic indenter this was not obvious, as the dimensions of the indentations were very small compared to the other tests.

In order to check the validity of the above results, it is necessary to compare the experimental results to the theory.

Figure 7.4 shows the theoretical curves for a sphere obtained from equation 5.14 where Young's modulus of the specimen is taken as 75 GPa for soft metals (aluminium) and 200 GPa for the steels. The experimental results are superimposed on the curves to graphically represent the correlation.

Figure 7.5 uses the same parameters in conjunction with equation 6.14 to demonstrate a similar correlation for cones.

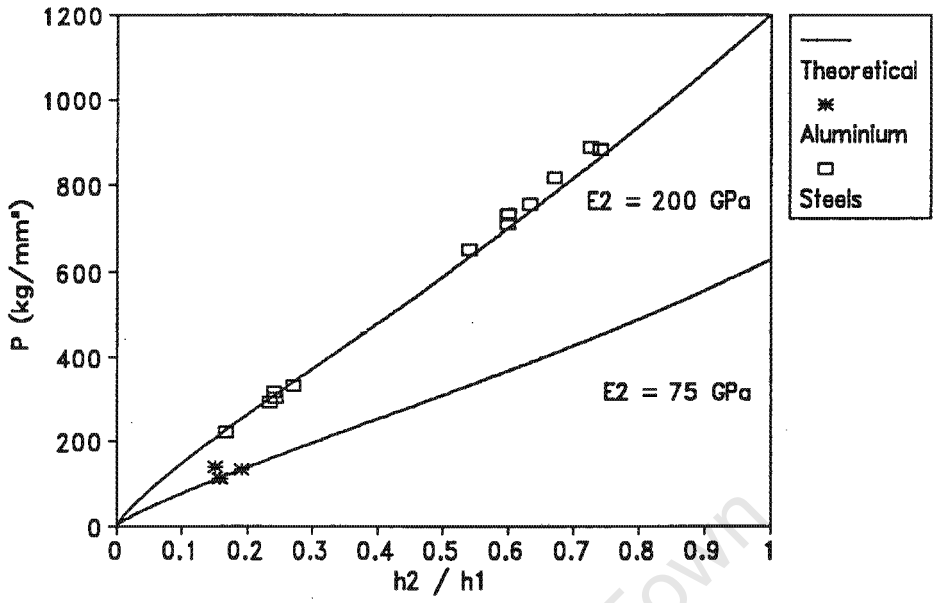

Fig 7.4 Theoretical and Experimental Dynamic Yield Pressure of a Sphere against the ratio of Rebound Height divided by Initial Height

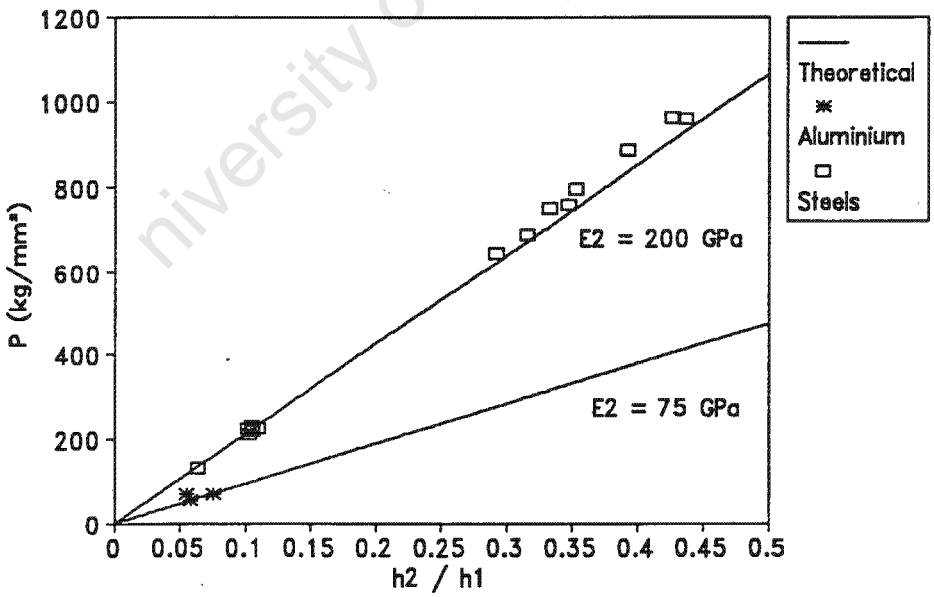

Fig 7.5 Theoretical and Experimental Dynamic Yield Pressure of a Cone against the ratio of Rebound Height divided by Initial Height

For clarity, the results of the static and dynamic tests are shown in table 7.2. Where $H = h_2 / h_1$

Table 7.2

Summary of Results

Spec	HV 30	HB	HRC	HRB	H_{cone}	H_{sphere}
A	203	193	—	94	0.105	0.270
B	800	—	64	—	0.393	0.670
C	638	—	57	—	0.353	0.598
D	195	185	—	93	0.109	0.243
E	550	—	53	—	0.316	0.598
F	480	—	48	—	0.292	0.540
G	850	—	66	—	0.437	0.740
H	630	—	57	—	0.347	0.633
1	135	128	—	75	0.075	0.190
2	110	107	—	61	0.058	0.157
3	98	95	—	51	0.055	0.150
4	120	120	—	66	0.063	0.166
5	205	195	—	95	0.104	0.246
6	204	194	—	94	0.101	0.240
7	180	170	—	89	0.102	0.234
8	108	104	—	59	0.058	0.156
9	640	—	58	—	0.333	0.600
10	820	—	65	—	0.427	0.726

The results are shown graphically in figures 7.6 to 7.9. A polynomial regression was carried out on each set of data and a best fit curve is given for each. The standard error of the estimate is also computed in order to give a confidence level in the regression analysis. The results are those of the averaged tests (5 tests per specimen) and thus do not show the scatter associated with each individual result. This would have resulted the in the figures being cluttered with too much data.

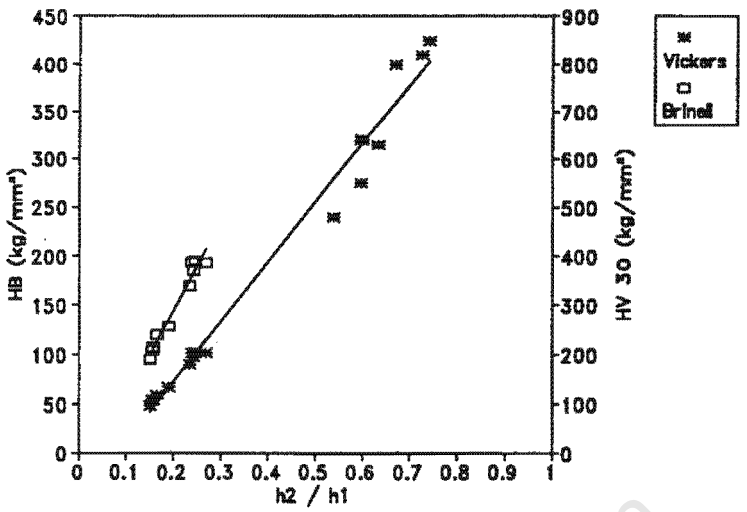

Fig 7.6 Vickers and Brinell Hardness Numbers against the ratio of Rebound Height divided by Initial Height of a Sphere

$$HV\ 30 = 1205\ H^{1.30} \pm 50 \qquad (7.1)$$

$$HB = 1092\ H^{1.26} \pm 20 \qquad (7.2)$$

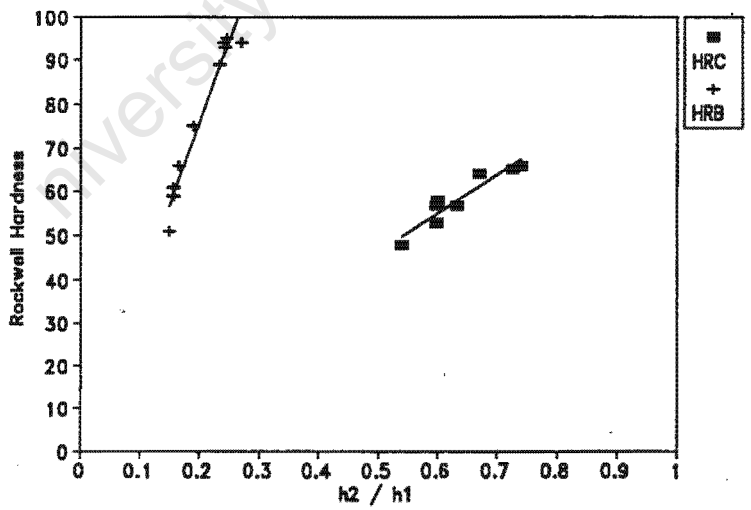

Fig 7.7 Rockwell B & C Hardness Numbers against the ratio of Rebound Height divided by Initial Height of a Sphere

$$HRB = 380\ H \pm 4 \qquad (7.3)$$

$$HRC = 89\ H \pm 2 \qquad (7.4)$$

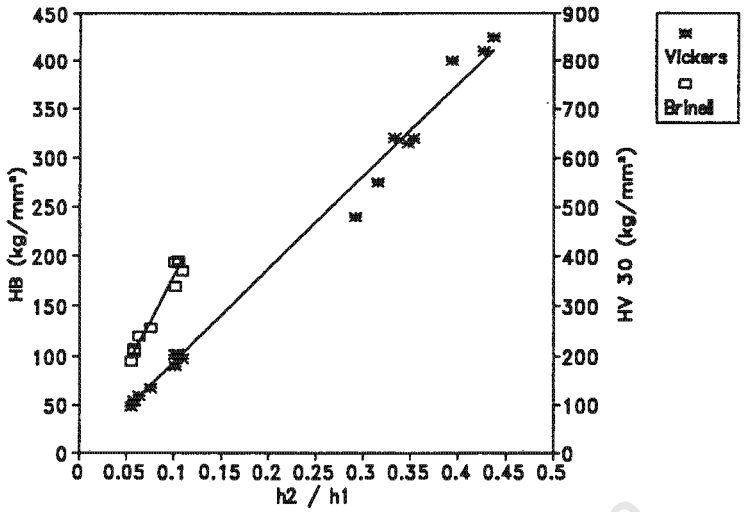

Fig 7.8 Vickers and Brinell Hardness Numbers against the ratio of Rebound Height divided by Initial Height of a Cone

$$\text{HV } 30 = 1880\,H \pm 30 \qquad (7.5)$$

$$\text{HB} = 1700\,H \pm 10 \qquad (7.6)$$

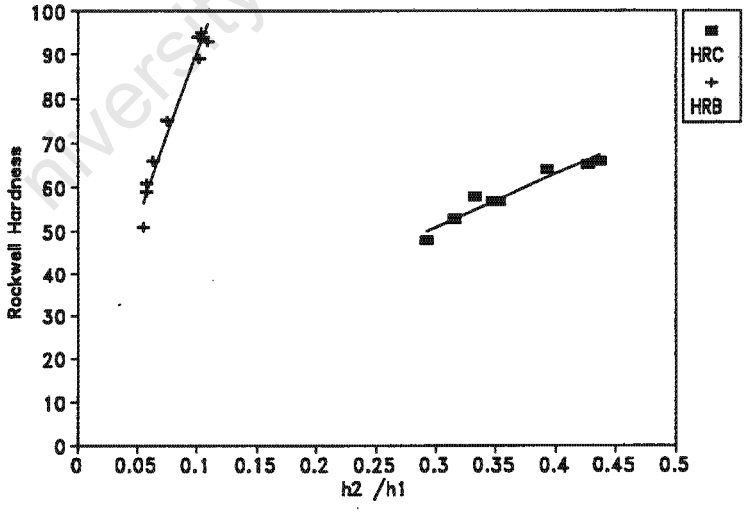

Fig 7.9 Rockwell B & C Hardness Numbers against the ratio of Rebound Height divided by Initial Height of a Cone

$$\text{HRB} = 562\,H^{0.75} \pm 3 \qquad (7.7)$$

$$\text{HRC} = 124\,H^{0.75} \pm 2 \qquad (7.8)$$

8. CONCLUSIONS

The design for a portable dynamic hardness tester based on a bouncing indenter has been developed. A brief discussion relating hardness to important material properties such as fatigue, creep and tensile strength is also given.

The more common static hardness tests (Brinell, Vickers and Rockwell) were studied and an understanding of the principles involved in the indentation process gained. Each test was critically examined to determine its advantages and limitations. The correlation between the hardness tests was also studied, since not all hardness scales (notably Rockwell) can be used in calculations to determine other properties such as tensile or yield strength as these numbers are dimensionless. It was determined that these empirical correlations are crude and the most accurate way of converting from one scale to another is by using empirical data from a source such as SABS 055 - 1977. A series of test specimens was produced and the above static hardness tests were carried out on to validate the correlations.

Since all the static tests have the disadvantage of having to be carried out in a laboratory or workshop, it was decided that the most viable option to carry out hardness tests *in situ* would be a dynamic hardness test. The most widely documented dynamic hardness test is the Shore scleroscope; this method has severe limitations however, amongst which are that the tester must be in a near perfectly vertical position. The test is more susceptible to variations in surface finish that other tests. Skilled operators are also needed for the accuracy of the readings, and lastly, the diamond tip is more prone to damage than the indenters of other testers.

The developed dynamic tester overcomes some of these problems by using an electronic measuring device to determine the height of rebound. The tip of the indenter is made of tungsten carbide to prevent damage, and if damage occurs, it may be quickly dressed to prevent lengthy repair times. The design of the indenter also allows the machining of a second tip at the free end of the shaft so that the operator has a spare tip at hand should the present one become damaged. Since the measuring of the height of rebound is electronic, it is quick and thus many tests may be made in a short period of time. This overcomes the problems of surface imperfections to a large extent since the results may be averaged. The shaft is in contact with the bearings at all times and thus the tester is not as sensitive to

inclinations from the vertical position as is the scleroscope. This problem could be further overcome by the use of a spring - loaded indenter in which the velocities rather than the heights are measured.

A study of the effects of using different indenter tips is also done. The theory of spherical and conical tips is discussed and comparisons drawn between the two. Experiments were carried out with the two different configurations and the results compared. Since these tests were done on the same test specimens which were used to compare the various static hardness values, a relationship between dynamic and static numbers was also determined. The correlations are based on curve fitting and are thus subject to the errors inherent in such procedures. The regression error analysis done on the data shows, however that the empirical curve fitting is in the order of 96 percent accurate. This indicates that the results obtained are consistent and repeatable which are two important criteria when judging material testing procedures.

These relationships were then programmed into the tester. The dynamic tester does thus not give an arbitrary number, but instead gives the operator the choice of having the results in the Vickers, Brinell, Rockwell C or Rockwell B scales.

Although the spherically tipped indenter was less prone to damage than the conically tipped one, the cone is more user friendly. It is easier to grind the desired angle onto the shaft than it is to grind a hemisphere. Also, the experiments done on the specimens have consistently shown that the results obtained from the conical tip are more accurate than those obtained from the sphere. This may be deduced since the error in the results for the spherical tip as shown in figures 7.6 to 7.9 are greater than those for the conical tip.

Another advantage of the conical tip is that it requires a lower initial height to produce plastic flow of the metal around the indenter and still give legitimate results. The significance of this is that the support of the test piece is of less importance to results. A loosely supported test piece gives erratic results and thus reduces the level of confidence in the test. Since the energy of impact of the conical indenter is lower than that of the spherical one, the support of the test piece is not as critical. This is also of importance if the test is carried out *in situ*. Lighter

impact loads require less parent metal on a specimen to produce consistent results. This means that the conical tip may be used on smaller fragments of material.

The recommendations which follow are given as a guideline to eliminate or at least reduce the sources of error involved in using the dynamic tester. If they are followed, the tester may be used with the same degree of confidence as that involved with static tests, but without their disadvantages.

9. RECOMMENDATIONS

The following recommendations are made for furthering the thesis procedure:

- Modify the tester to allow the measurement of velocities of descent and rebound instead of the height.

- Develop a spring loaded indenter to allow measurements to be made in a non - vertical position.

- Investigate further the influences of changing the initial height h_1 and the radius or angle of the tip of the indenter.

- Investigate the relationship between the hardness of the metal and other properties such as fatigue, creep and wear.

- Investigate further the effects of surface finish and morphology for small indentations.

- Investigate the relationship between ϵ_p and the ratio d/D as given by equation 3.11 as tests by Au et al [Au, 1980] have shown there to be a discrepancy between their results and Tabor's work.

The following recommendations are made concerning the use of the dynamic tester:

Conclusions and Recommendations

- For the accurate results ensure the specimens have two parallel ground faces.

- Preferably use specimens of consistent dimensions (60 x 20 x 20 mm) for accurate results.

- Avoid the testing of specimens above a hardness value of 800 H_V ($\pm$ 65 R_C) to prevent premature wear of the tip.

- Wherever possible, perform the test on the base provided in order to give consistent values.

- Apply a small amount of grease between the specimen and the base to prevent vibration of the specimen, as the vibrations lead to inconsistent results.

- Ensure that the shaft and the bearings as always clean for consistent results.

- Regularly inspect the tip of the indenter to ensure no damage has occurred as this will affect the measurements. Dress as necessary.

10. REFERENCES

A S T M (1983): Standard Test Method for Wear Testing With a Crossed-Cylinder Apparatus. Dec. 30.

Atkins A G & Tabor D (1965): Plastic Indentation of Metals with Cones. J. Mech. Phys. Solids, Vol.13, pp. 149 to 164. Pergamon Press Ltd.

Au P, Lucas G E, Sheckherd J W & Odette G R (1980): Flow Property Measurements from Instrumentated Hardness Tests. Nondestructive Evaluation in the Nuclear Industry - 1980. Proc 3rd Int. Conf. ASM.

Böklen R (1971): A Simple Method for Obtaining the Ductility from a 100° Cone Impression. The Science of Hardness Testing and its Research Applications. ASM.

Bowden F P & Tabor D (1968): The Friction and Lubrication of Solids. Part II Claredon Press: Oxford.

Brinell J A (1900): Congrès International des Methodes d'Essai, Paris.

BS 240 (1968): Determination of Brinell Hardness: Part 1.

BS 891 (1962): Rockwell Hardness Test: Part 1.

Cahoon J R (1972): An Improved Equation Relating Hardness to Ultimate Strength. Metallurgical Transactions, Volume 3, ASM and AIME.

Cane B J, Aplin P F & Brear J M (1985): A Mechanistic Approach to Remnant Creep Life Assessment of Low Alloy Ferritic Components Based on Hardness Measurement. Journal of Pressure Vessel Technology, Vol 107, August.

Davis H E, Troxel G E & Wiskocil C T (1964): The Testing and Inspection of Engineering Materials. McGraw-Hill Book Company.

De La Macorra F (1923): Relation beteen the Rockwell and Brinell Numeral for Testing Hardness of Metal. B.S. Thesis, M.I.T., Cambridge, Mass.

Edwards C A & Austin C R (1923): J. Iron & Steel Inst. 107, 324.

Francis H A (1976): Phenomenological Analysis of Plastic Spherical Indentation. Trans. ASME, p. 272.

Hertz H (1881): J. reine angew. Math. 92, 156.

Hill R (1950): The Mathematical Theory of Plasticity. Claredon Press, Oxford.

Jankowski D (1988): Hardness Testing Makes an Impression. Quality Progress. Oct 1988.

References

Janna W S (1988): Engineering Heat Transfer. SI Edition. Van Nostrand Reinhold (International).

Johnson K L (1970): The Correlation Of Indentation Experiments. J. Mech. Solids, vol. 18, pp. 115 to 126. Pergamon Press.

Kimura K, Fujiyama J, Ishii F & Muramatsu M (1990): Effect of Material Degradation on Creep Properties and Life Estimation. Toshiba Corporation, Yokohama, Japan.

Liddicoat R T & Potts P O (1952): Laboratory Manual of Materials Testing. The Macmillan Company New York.

Lipson C (1967): Wear Considerations in Design. Prentice-Hall, Inc. N.J.

Lockett F J (1963): J. Mech. Phys. Solids 11, 345.

Martell R (1895): Commission de Methodes d'Essai des Materiaux de Construction. 3, 261, Paris.

McClintock F A & Argon A S (eds) (1966): Mechanical Behaviour of Materials. Addison-Wesley Publishing Company, Inc. Reading, Massachusetts, USA.

Meyer E (1908): Zeits. d. Vereins Deutsch. Ingenieure, 52, 645.

Moore H F (1947): Materials of Engineering. 7th ed. McGraw Hill Book Co.

Moteff J & Sieber P (1974): A Correlation between the Hot-Hardness and the Hot-Tensile Properties of AISI 304 Stainless Steel. Metallurgical Transactions, Volume 5.

Nadai A (1931): Plasticity. McGraw Hill, New York.

O'Neill H (1967): Hardness Measurement of Metals and Alloys. 2nd ed. Chapman and Hall Ltd.

Pugh B (1973): Friction and Wear. Newnes-Butterworths: London.

Rockwell S P (1922): The Testing of Metals for Hardness. Trans. Am. Soc. Steel Treat. 2, 1013 - 1033.

S A B S 055-1977: Methods of Hardness Testing of Metallic Materials.

Shabel B S & Young R F (1987): A Rapid Strength Determination Procedure for Metallic Alloys. Light Metal Age, June.

Shaw M C & De Salvo G J (1970): On Plastic Flow beneath a Blunt Axisymmetric Indenter. Trans. ASME, p. 482.

Shigley J E & Mitchell L D (1984): Mechanical Engineering Design McGraw Hill.

References

Shore A F (1918): Journal of Iron & Steel Inst. 2, 59.

Stilwell N A & Tabor D (1961): Elastic Recovery of Conical Indentations. Phys. Proc. Soc. 528, 2.

Tabor D (1951): The Hardness of Metals. Claredon Press.

Timoshenko S and Goodier J N (1970): Theory of Elasticity, McGraw Hill New York.

Ugural A & Fenster S K (1981): Advanced Strength and Applied Elasticity : The S I Version, Edward Arnold, London.

Williams S R (1942): Hardness and Hardness Measurements. A S M, Cleveland, Ohio.

Woehler A (1871): Engineering, London, Vol. 11.

Zienkiewicz O C & Holister G S (1965): Stress Analysis, John Wiley and Sons, London, University Press.

APPENDIX A

This appendix shows photographs and a schematic of the portable hardness tester.

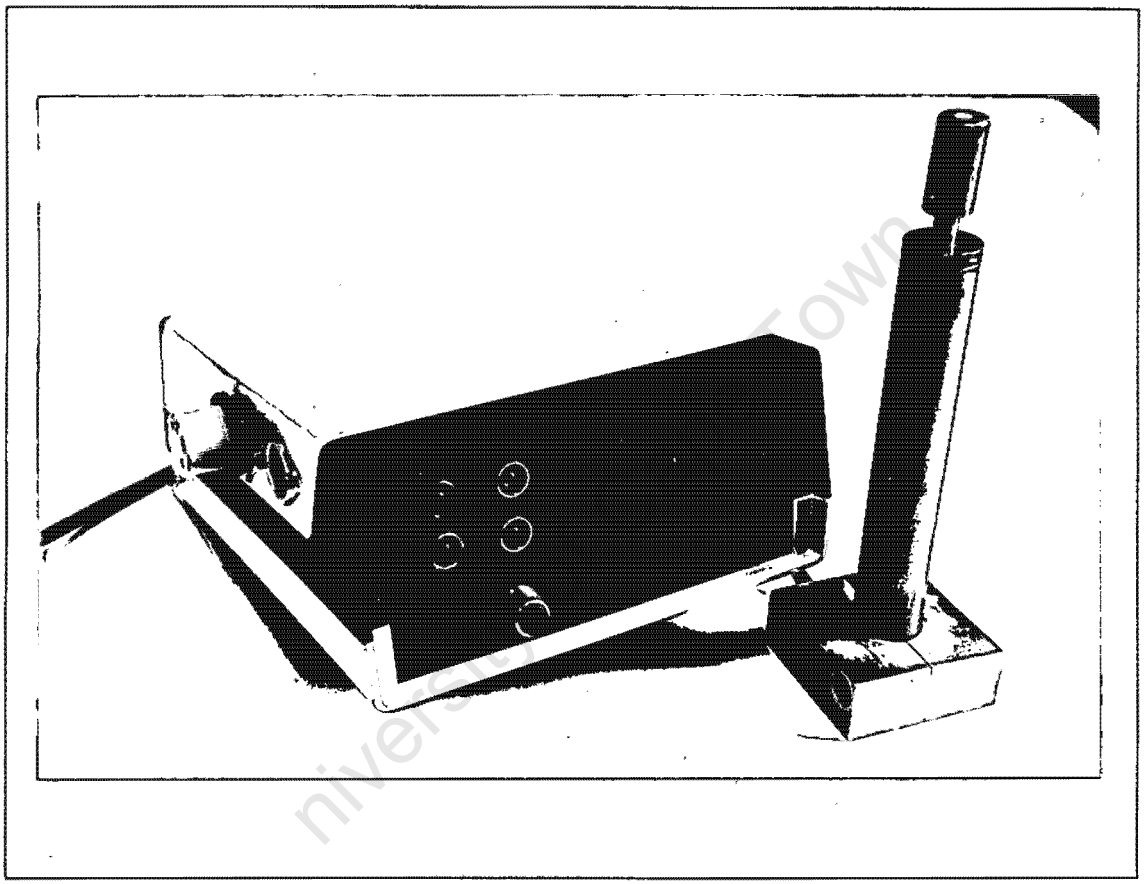

Figure A 1 View of the Tester Assembly

Appendix A

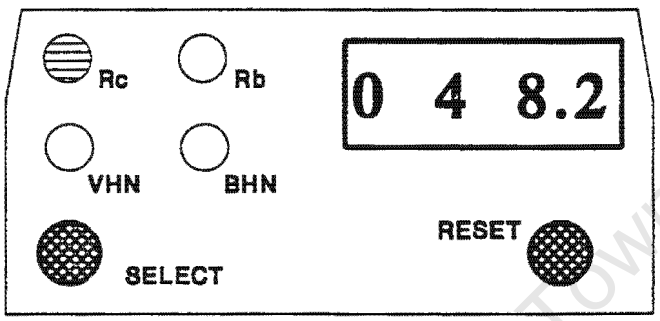

Figure A 2 Schematic of the Control Panel Layout

APPENDIX B

Appendix B shows the relevant material properties of the indenter and the specimens. It also shows how they were obtained.

B 1 INDENTER PROPERTIES

Material:	Tungsten Carbide
Density (ρ):	14796 kg/m^3
Young's Modulus (E):	601 GPa

B 2 SPECIMEN PROPERTIES

The Young's modulus of the indenter and the specimens was determined with the help of professor Bell of the department of electrical engineering. The following procedure was used to determine the modulus.

1. A sonic pulse was transmitted along the specimen.
2. The velocity of sound in the metal was then measured.
3. The modulus was then calculated from the following formula:

$$E = c^2 \varpi \qquad \text{(B 1.0)}$$

Where:
c is the speed of sound in the metal.
ϖ is the resonant frequency of the specimen.

Appendix B

Specimen	Material	Density (ρ) (kg/m^3)	Young's Modulus (E) (GPa)
A	BMS	7753	193
B	Carbon Steel	7801	216
C	Carbon Steel	7801	216
D	Mild Steel	7753	193
E	Hardened Steel	7871	206
F	Hardened Steel	7459	210
G	Tool Steel	7785	208
H	Tool Steel	7806	208
1	Aluminium	2787	75
2	Aluminium	2787	75
3	Aluminium	2787	75
4	Brass	8522	106
5	Mild Steel	7753	193
6	Steel	7801	210
7	Stainless Steel	7817	190
8	Aluminium	2787	75
9	Carbon Steel	7753	216
10	Carbon Steel	7753	216

APPENDIX C

Appendix C shows the results of the dynamic hardness tests performed on the specimens. The tests were performed with a spherical and a conically tipped indenter.

The dynamic hardness tester was so constructed as to measure the time of rebound of the indenter. This time of rebound was then used to calculate the height of rebound h_2. Newton's laws were used for this purpose. Since the time for the drop and the rebound are measured, it is assumed that $time_{up} = time_{down}$ and hence the time used for the calculation is actually $(time_{measured})/_2$. Thus

$$S = ut + \tfrac{1}{2} gt^2 \qquad \text{(C 1.0)}$$

Where:
S = distance
u = initial velocity = 0
t = time
g = acceleration due to gravity

and thus equation (C1.0) becomes

$$h_2 = {}^1/_8 \, g \, t^2_{measured} \qquad \text{(C1.1)}$$

C 1 SPHERICALLY TIPPED INDENTER

Indenter Mass:	70.68 E-03 kg
Indenter Density:	14796 kg/m^3
Length:	153 E-03 m
Diameter of Shaft:	6.35 E-03 m
Radius of tip (r_1):	3.175 E-03 m
Initial Height:	60 E-03 m

Appendix C

Specimen	Time of Rebound (ms)	Height of Rebound (mm)	Height of Rebound (h_2) / Initial Height (h_1)
A	114.9	16.20	0.270
B	181.1	40.20	0.670
C	171.1	35.88	0.598
D	109.0	14.58	0.243
E	171.1	35.88	0.598
F	162.5	32.40	0.540
G	190.3	44.40	0.740
H	176.0	37.98	0.633
1	96.4	11.40	0.190
2	87.6	9.42	0.157
3	85.7	9.00	0.150
4	90.1	9.96	0.166
5	109.7	14.76	0.246
6	108.4	14.40	0.240
7	107.0	14.04	0.234
8	87.4	9.36	0.156
9	171.3	36.00	0.600
10	188.5	43.56	0.726

Appendix C

C 2 CONICALLY TIPPED INDENTER

Indenter Mass:	89.6 E-03 kg
Indenter Density:	14796 kg/m^3
Length:	153 E-03 m
Diameter of Shaft:	6.35 E-03 m
Cone Angle :	136°
Initial Height:	42 E-03 m

Specimen	Time of Rebound (ms)	Height of Rebound (mm)	Height of Rebound (h_2) / Initial Height (h_1)
A	60.0	4.41	0.105
B	116.0	16.51	0.393
C	110.0	14.83	0.353
D	61.1	4.58	0.109
E	104.0	13.27	0.316
F	100.0	12.26	0.292
G	122.3	18.35	0.437
H	109.0	14.57	0.347
1	50.7	3.15	0.075
2	44.6	2.44	0.058
3	43.4	2.31	0.055
4	46.5	2.65	0.063
5	59.7	4.37	0.104
6	58.8	4.24	0.101
7	59.1	4.28	0.102
8	44.6	2.44	0.058
9	106.8	13.99	0.333
10	120.9	17.93	0.427

APPENDIX D

This appendix shows the results of standard hardness tests carried out on the control specimens to calibrate the hardness tester. The tests were carried out on the Rockwell tester belonging to the department of Mechanical Engineering and on the universal hardness tester of the department of Materials Engineering of the University of Cape Town.

	ROCKWELL C	ROCKWELL B	VICKERS kg/mm²	BRINELL kg/mm²
Specimen				
A	—	94	203	193
B	64	—	800	—
C	57	—	638	—
D	—	93	195	185
E	53	—	550	—
F	48	—	480	—
G	66	—	850	—
H	57	—	630	—
1	—	75	135	128
2	—	61	110	107
3	—	51	98	95
4	—	66	120	114
5	—	95	205	195
6	—	94	204	194
7	—	89	180	170
8	—	59	108	104
9	58	—	640	—
10	65	—	820	—

APPENDIX E

Appendix E shows drawings of the indenter shaft, housing and base.

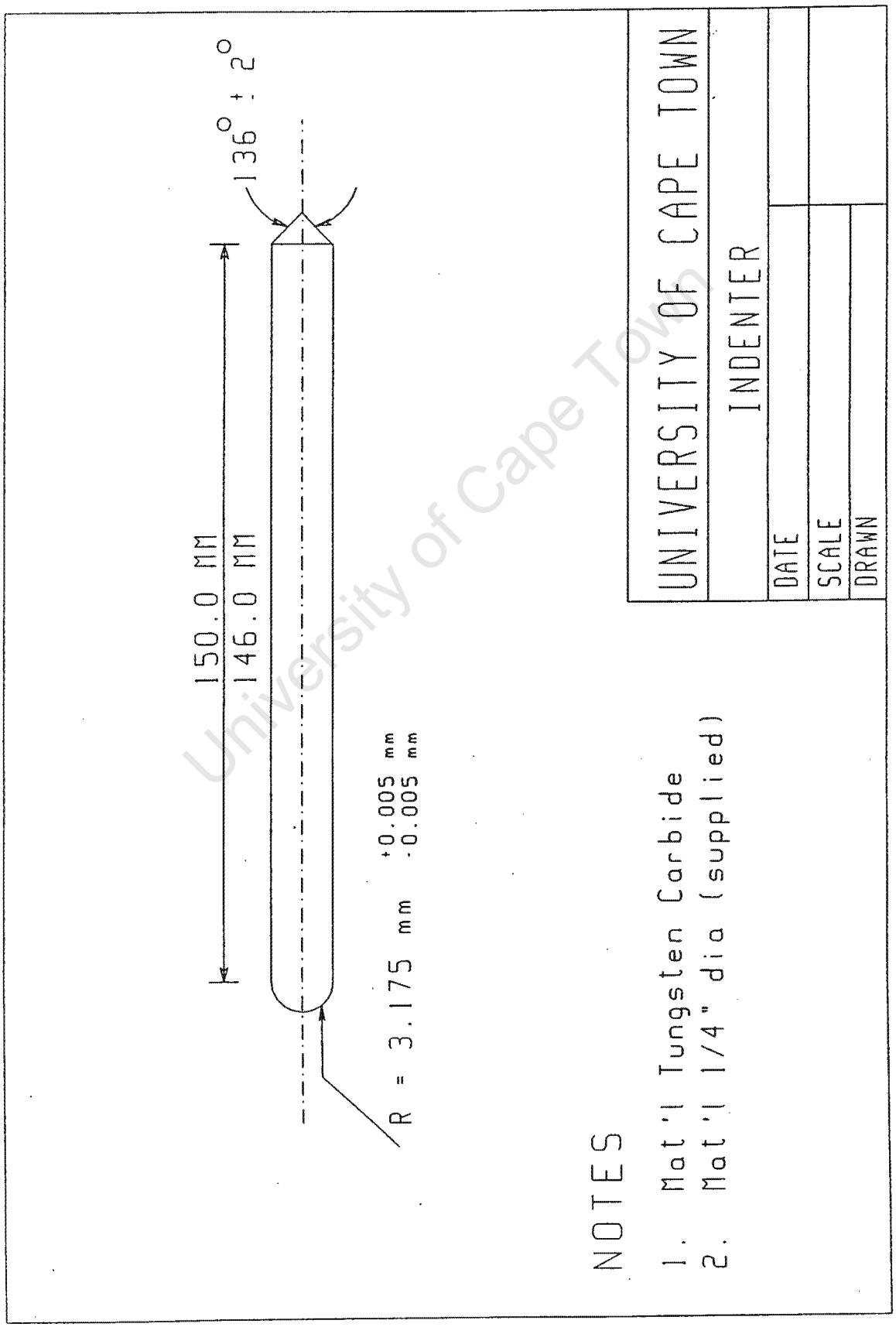

NOTES

1. Mat'l Aluminium
2. Anodise Black

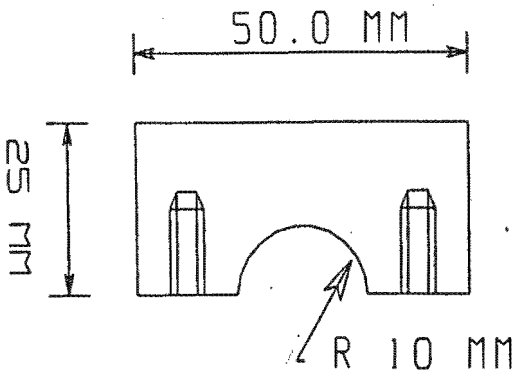

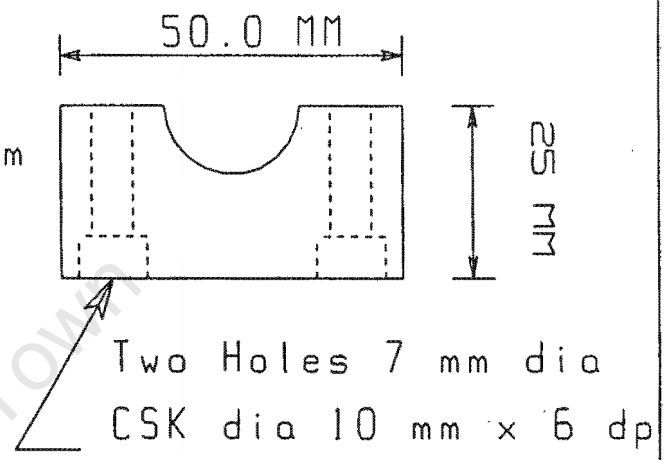

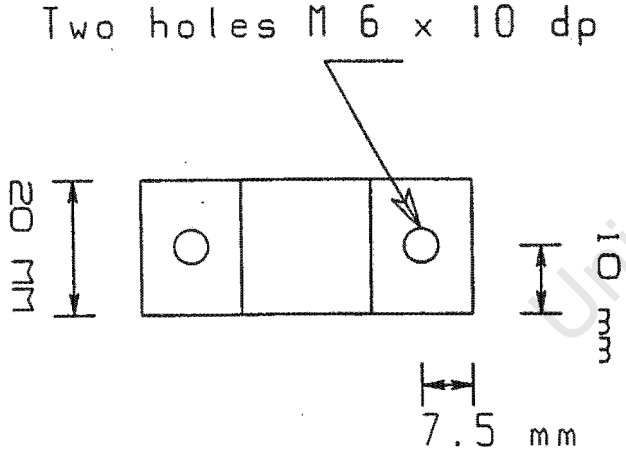

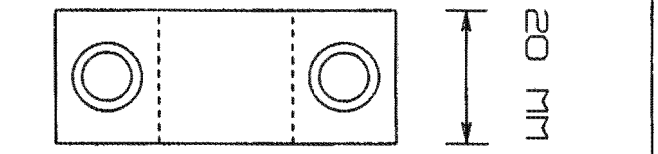

UNIVERSITY OF CAPE TOWN	
BASE	
DATE	
SCALE 1 1	
DRAWN	

Mat'l BMS
Finish Chrome Plate

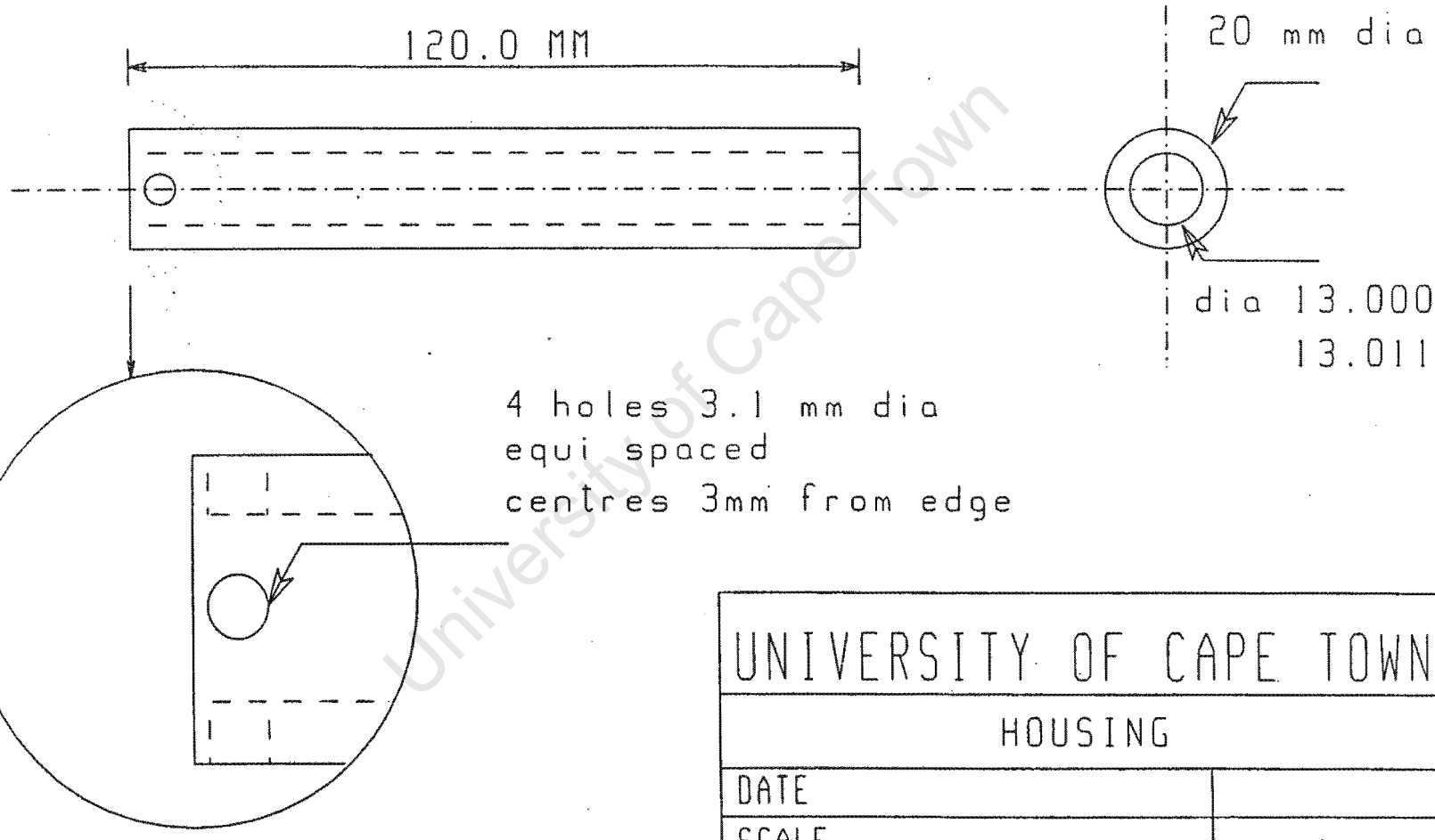

UNIVERSITY OF CAPE TOWN	
HOUSING	
DATE	
SCALE	
DRAWN	

Appendix E

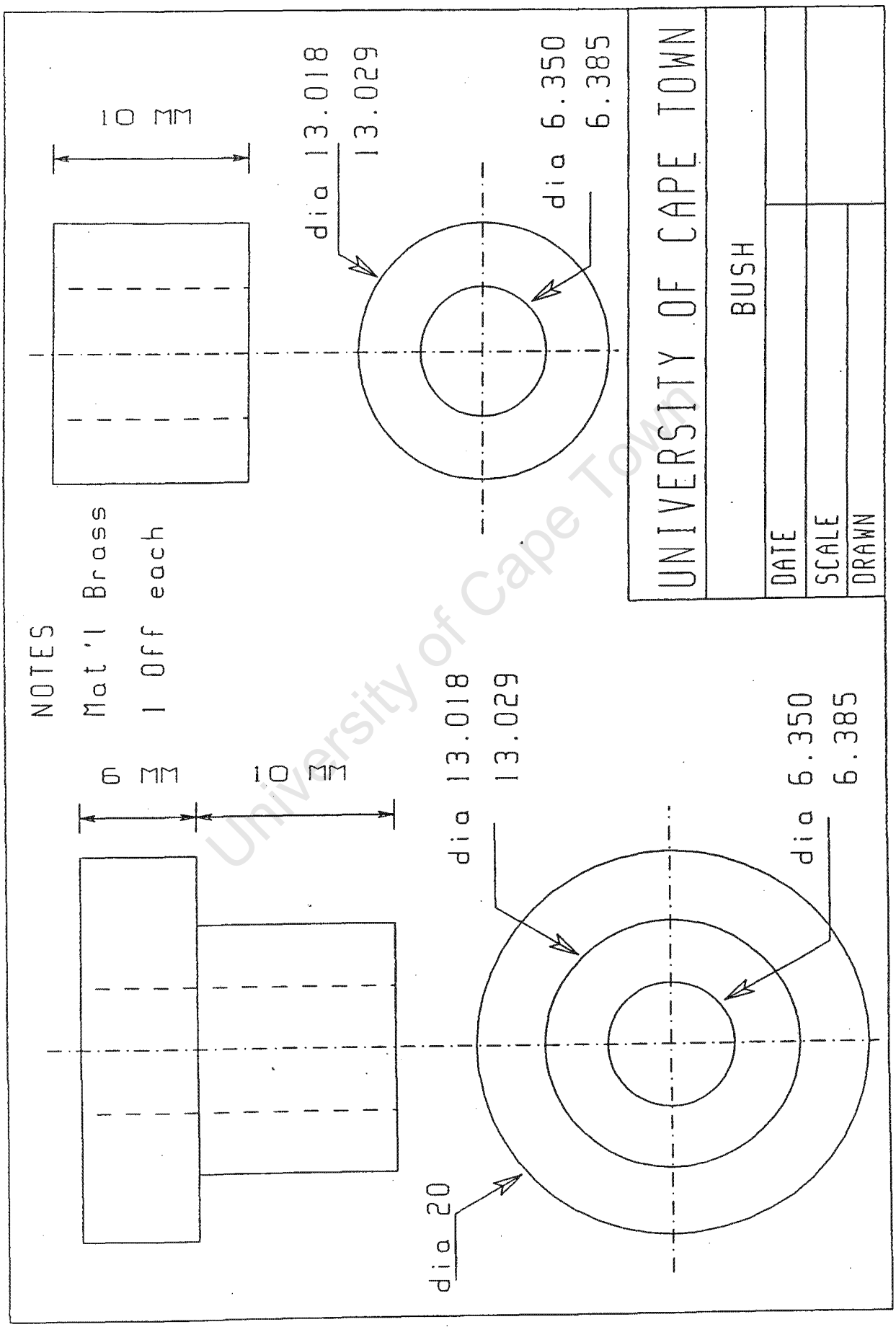

APPENDIX F

Appendix F shows examples of the results obtained from dynamic tests carried out with a conical tip on standard calibration specimens. The results are analysed and the same procedure is used on each specimen to calibrate the tester. Specimens B and D are used as examples for steels and specimen 1 for the aluminium. These are chosen, since the specimens for steel show that the statistical analysis is valid at the lower and upper ranges of the test. In other words, the deviations from the mean are similar in both cases. Since all the aluminium specimens had similar hardness, number 1 was chosen for the analysis.

Specimen	Time (ms)	Analysis Results
B	117.4	
	116.0	
	116.5	
	115.7	Mean: 116.0
	114.6	Std dev: 1.03
D	60.5	
	61.3	
	60.8	
	62.3	Mean: 61.1
	60.2	Std dev: 0.82
1	51.0	
	52.8	
	49.3	
	49.6	Mean: 50.8
	51.4	Std dev: 1.42

After the calibration had been carried out, and the tester programmed, tests were then carried out on a test specimen with a ground surface. This was done in order to determine how many tests should be performed on a specimen before an average hardness for that specimen could be determined with an acceptable level of confidence. The block was of the dimensions found in the recommendations and placed on the base provided. The following results were obtained using the

Appendix F

Rockwell C scale on the indenter. The block was then subjected to the standard Rockwell test and a result of 59 R_c was recorded.

Test No.	Hardness Value (R_c)
1	58.2
2	60.0
3	58.2
4	61.9
5	59.1
6	60.0
7	59.1
8	61.9
9	59.1
10	61.9

The mean value of all ten readings is 59.9 R_c with a standard deviation of 1.5 R_c. If one takes the first five readings and performs a similar statistical analysis, the mean value is 59.5 R_c with a standard deviation of 1.5 R_c. Again performing the analysis on the second five readings gives a result of 60.4 R_c with a standard deviation of 1.4 R_c. These tolerances fall within those set out for standard Rockwell tests, but looking at the table of results, the minimum value is 58 R_c and the maximum 62 R_c. For this reason, it is suggested that at least five tests be performed in order to obtain a hardness value conforming to industry standards.